PALEOCEANOGRAPHY, VOL. 21, PA2020, doi:10.1029/2005PA001166, 2006

Decadal cyclicity of regional mid-Holocene precipitation: Evidence from Dominican coral proxies

Lisa Greer[1] and Peter K. Swart[2]

Received 8 April 2005; revised 1 February 2006; accepted 14 February 2006; published 29 June 2006.

[1] The stable carbon ($\delta^{13}C$) and oxygen ($\delta^{18}O$) isotopic compositions of four Holocene specimens of *Montastraea sp.* and *Siderastrea sp.* coral skeletons from the Dominican Republic were analyzed to examine decadal-scale fluctuations in regional precipitation. The specimens range in length from 47 to 197 years individually and range in age from ~7.2 to 5.2 kyr. Oscillations in the $\delta^{13}C$ and $\delta^{18}O$ of coral skeletons from the Holocene Enriquillo Valley occur with a seemingly consistent frequency of 15–20 years. For one coral (~6 ka) this decadal to multidecadal mode of variability is statistically significant. The decadal to multidecadal mode of stable isotopic variability may represent cyclic fluctuations in mid-Holocene migration of the Intertropical Convergence Zone (ITCZ) or in the hydrogeology of the region as governed by fluctuations in the passage of tropical storms and hurricanes. Regional temperature is believed to act as only a secondary control on the $\delta^{18}O$ values of these corals. However, ITCZ migration and/or oscillations in storm frequency at this site may ultimately reflect decadal-scale patterns in greater tropical North Atlantic sea surface temperatures. The length and resolution of climate variability represented in this study indicate a persistent decadal to multidecadal mode of Atlantic climate fluctuation throughout the mid-Holocene that is indistinguishable from observed historical climate.

Citation: Greer, L., and P. K. Swart (2006), Decadal cyclicity of regional mid-Holocene precipitation: Evidence from Dominican coral proxies, *Paleoceanography*, *21*, PA2020, doi:10.1029/2005PA001166.

1. Introduction

1.1. Atlantic Decadal Climate Variability

[2] Cycles in climate variability occur on scales that range from subannual to at least multimillennial in frequency. The forces behind observed decadal climate phenomena in the Atlantic are complex and frequently debated [e.g., *Hurrell*, 1995; *Carton et al.*, 1996; *Hurrell and Vanloon*, 1997; *Chang et al.*, 1997; *Enfield and Mayer*, 1997; *Marshall et al.*, 2001; *Dong and Sutton*, 2003; *Joyce et al.*, 2004; *Huang et al.*, 2004]. Decadal and centennial climate variability may be forced by a number of potential mechanisms, depending on local, regional, and global patterns in weather, insolation, and geography.

[3] Observed climate patterns in the tropical Atlantic include decadal to multidecadal patterns (here defined as 12–20 years) in (1) Atlantic sea surface temperature (SST) anomalies [*Carton et al.*, 1996; *Chang et al.*, 1997; *Marshall et al.*, 2001], (2) precipitation off the west coast of Africa [*Gray et al.*, 1997], and (3) Atlantic tropical storm frequency [*Landsea et al.*, 1992; *Zhang et al.*, 2000; *Elsner et al.*, 2000]. In particular, several studies cite an observed 12–15 year frequency of SST variability in the tropical Atlantic [*Chang et al.*, 1997; *Moron et al.*, 1998; *Hakkinen*, 2000; *Joyce et al.*, 2000; *Cobb et al.*, 2001] and the Western Hemisphere Warm Pool [*Wang and Enfield*, 2001]. This decadal pattern in SST, sometimes thought to exist as a function of dipole-like conditions in the tropical Atlantic, has been the focus of numerous observational and modeling studies, and there is much debate as to the mechanism(s) of decadal Atlantic climate variability [*Nobre and Shukla*, 1996; *Chang et al.*, 1997, 2000; *Tanimoto and Xie*, 2002; *Kushnir et al.*, 2002; *Huang et al.*, 2004; *Joyce et al.*, 2004].

[4] Most conceptual models of Atlantic climate point to a dynamic ocean as a participant rather than observer in ocean-atmosphere interactions, particularly on lower-frequency timescales. The mechanisms for decadal Atlantic climate change are likely forced by changes in insolation, surface or thermohaline circulation, or air-sea exchange of heat and energy. In addition to Atlantic origin climate forcing mechanisms, ENSO activity has documented teleconnections with Atlantic climate [*Gray*, 1984a; *Landsea et al.*, 1994; *Lighthill et al.*, 1994; *Chang et al.*, 2000; *Saravanan and Chang*, 2000]. While Pacific ENSO activity and precipitation patterns in the West African Sahel have been linked to patterns in the formation and intensity of Atlantic tropical storms and hurricanes on a decadal scale [*Gray*, 1984a, 1984b; *Landsea and Gray*, 1992; *Lighthill et al.*, 1994; *Landsea et al.*, 1996; *Gray et al.*, 1997], few high-resolution reconstructions of hurricane patterns predating historical records have been attempted [e.g., *Liu and Fearn*, 2001]. Historical records of Atlantic hurricane path, frequency and intensity exist only for the last century [*Neumann et al.*, 1993; *Landsea*, 1993].

1.2. Mid-Holocene Climate

[5] Many studies indicate that changes in insolation have profound effects on seasonal to millennial global climate

[1]Department of Geology, Washington and Lee University, Lexington, Virginia, USA.
[2]Rosenstiel School of Marine and Atmospheric Science, University of Miami, Miami, Florida, USA.

0883-8305/06/2005PA001166$12.00

patterns [*Rind and Overpeck*, 1994; *Lean and Rind*, 2001]. Early and mid-Holocene northern insolation was very different than at present. The mid-Holocene was a time of decreasing seasonal insolation in the Northern Hemisphere because of changes in the Earth's orbit [*Berger*, 1978] with the most rapid rate of insolation decline after ~6 ka [*Steig*, 1999]. Holocene changes in insolation may have resulted in dramatic spatial differences in surface heating and therefore ocean and atmospheric circulation.

[6] The mid-Holocene (here loosely defined as the period from 5–8 kyr) was a time of particularly rapid changes in global climate patterns [*Steig*, 1999]. Evidence exists for significant non-linear changes in mid-Holocene atmospheric and sea surface temperatures [*Bond et al.*, 1997; *Gagan et al.*, 1998; *Steig*, 1999], global oceanic and atmospheric circulation [*Steig*, 1999], North Atlantic Deep Water formation [*Charles et al.*, 1996], atmospheric trace gas levels [*Indermuhle et al.*, 1999], the frequency of storms and El Nino events [*Rodbell et al.*, 1999] and Pacific monsoon patterns [*Johnson et al.*, 1999].

[7] While there is abundant evidence for rising temperatures throughout most of the middle to late Holocene, changes in precipitation have been documented as well. The transition from the last Pleistocene glacial maximum to the early Holocene resulted in a globally synchronous change from dry and cool to warmer and more humid conditions. Mid-Holocene changes in precipitation, atmospheric circulation, and vegetation have been well documented in Africa and Central and South America [*Bradbury et al.*, 1981; *Piperno et al.*, 1990; *Peterson et al.*, 1991; *Hodell et al.*, 1995; *deMenocal et al.*, 2000; *Seltzer et al.*, 2000; *Black et al.*, 2004]. A distinct transition from arid to moist conditions in Central America, the Caribbean and Africa has been documented and termed the mid-Holocene moist, wet, warm or humid period [*Hodell et al.*, 1991; *deMenocal et al.*, 2000]. The onset and termination of this period appear to vary geographically.

[8] Proxy climate records from the Caribbean show late glacial arid conditions, a moist and warm mid-Holocene and a transition to more arid conditions in the late Holocene [*Bradbury et al.*, 1981; *Piperno et al.*, 1990; *Hodell et al.*, 1991; *Curtis and Hodell*, 1993]. Temporally well-constrained geochemical measurements [*Hodell et al.*, 1991; *Curtis and Hodell*, 1993] and pollen records [*Higuera-Gundy*, 1991] from a sediment core from Lake Miragoane (Haiti) provide proxy climate data geographically closest to the Enriquillo Valley, the site of this study. Analyses of the Lake Miragoane core ($\delta^{18}O$, Sr/Ca, pollen) indicate concomitant increases and decreases in both temperature and precipitation during the mid-Holocene [*Hodell et al.*, 1991; *Curtis and Hodell*, 1993; *Higuera-Gundy*, 1991]. *Hodell et al.* [1991] and *Curtis and Hodell* [1993] observed transitions in the $\delta^{18}O$ of ostracods from Lake Miragoane sediments interpreted to represent changes in the evaporation/precipitation balance for the Caribbean. Data from Miragoane show dry conditions (enriched $\delta^{18}O$) from 10.5 to 10.0 kyr with an increase in moisture (progressive depletion of $\delta^{18}O$) from ~10 to 7 kyr. The most depleted $\delta^{18}O$ values occurred from ~7.0 to 5.3 kyr, after which a slight enrichment in $\delta^{18}O$ was interpreted to signal a decrease in moisture [*Hodell et al.*, 1991; *Curtis and Hodell*, 1993]. The enrichment in $\delta^{18}O$ of the Miragoane core at ~5.3 ka roughly coincides with the abrupt termination of the African Humid Period ~5.5 ka [*deMenocal et al.*, 2000, and references therein].

1.3. Corals as Climate Proxies

[9] Many coupled ocean and atmospheric models of past tropical Atlantic climate rely on verification using historic SST data that rarely extend beyond the last century. Therefore the accuracy of such models, in defining conditions for longer time periods, is limited by a lack of data. Despite the short length of available SST chronologies from the tropical Atlantic, some interannual patterns in SST variability appear to be significant. Proxy records of climate potentially extend the record of decadal Atlantic climate fluctuations beyond the last century.

[10] The geochemical compositions of scleractinian corals have long been used as proxy records of climate. Valuable information concerning the environment in which a coral grew is recorded within the chronology of changing geochemical composition of coral skeletal carbonate. It has been shown that the $\delta^{13}C$, $\delta^{18}O$, and trace element content of coral carbonate can reflect key marine environmental parameters during coral growth. Corals can therefore serve as proxy records of various components of the climate system, including sea surface temperatures [*Weber and Woodhead*, 1972; *Fairbanks and Dodge*, 1979; *Beck et al.*, 1992; *Dunbar and Wellington*, 1981] and patterns in precipitation and evaporation [*Swart and Coleman*, 1980; *Cole and Fairbanks*, 1990; *Cole et al.*, 1993; *Gagan et al.*, 2000; *Swart et al.*, 2001; *Kilbourne et al.*, 2004] in local, regional, and global paleoclimate systems. Geochemical coral records have been instrumental in reconstructing paleo-ENSO activity [*Cole et al.*, 1993; *Dunbar et al.*, 1994; *Charles et al.*, 1997; *Linsley et al.*, 2000; *Le Bec et al.*, 2000; *Tudhope et al.*, 2001] and precipitation patterns in the West African Sahel [*Swart et al.*, 1998].

[11] This paper compares decadal patterns in climate between the present day and a four periods between ~7.2 and 5.2 kyr using historical climatological data and stable oxygen and carbon isotopic composition of corals from a Holocene locality in the Enriquillo Valley, Dominican Republic. A decadal to multidecadal-scale mode of variability in $\delta^{13}C$ and $\delta^{18}O$ data from Holocene Dominican corals is proposed to reflect decadal-scale changes in precipitation between ~7.2 and ~5.2 kyr. We propose that these patterns in Holocene precipitation may have been driven by changes in latitudinal migration of the Intertropical Convergence Zone (ITCZ) or storm activity, both of which may have ultimately been driven by fluctuations in tropical Atlantic SSTs.

2. Methods

2.1. Site Selection and Sample Collection

[12] The Enriquillo Valley is located in the southwestern interior of the Dominican Republic and trends approximately east to west from the Caribbean Sea in the Dominican

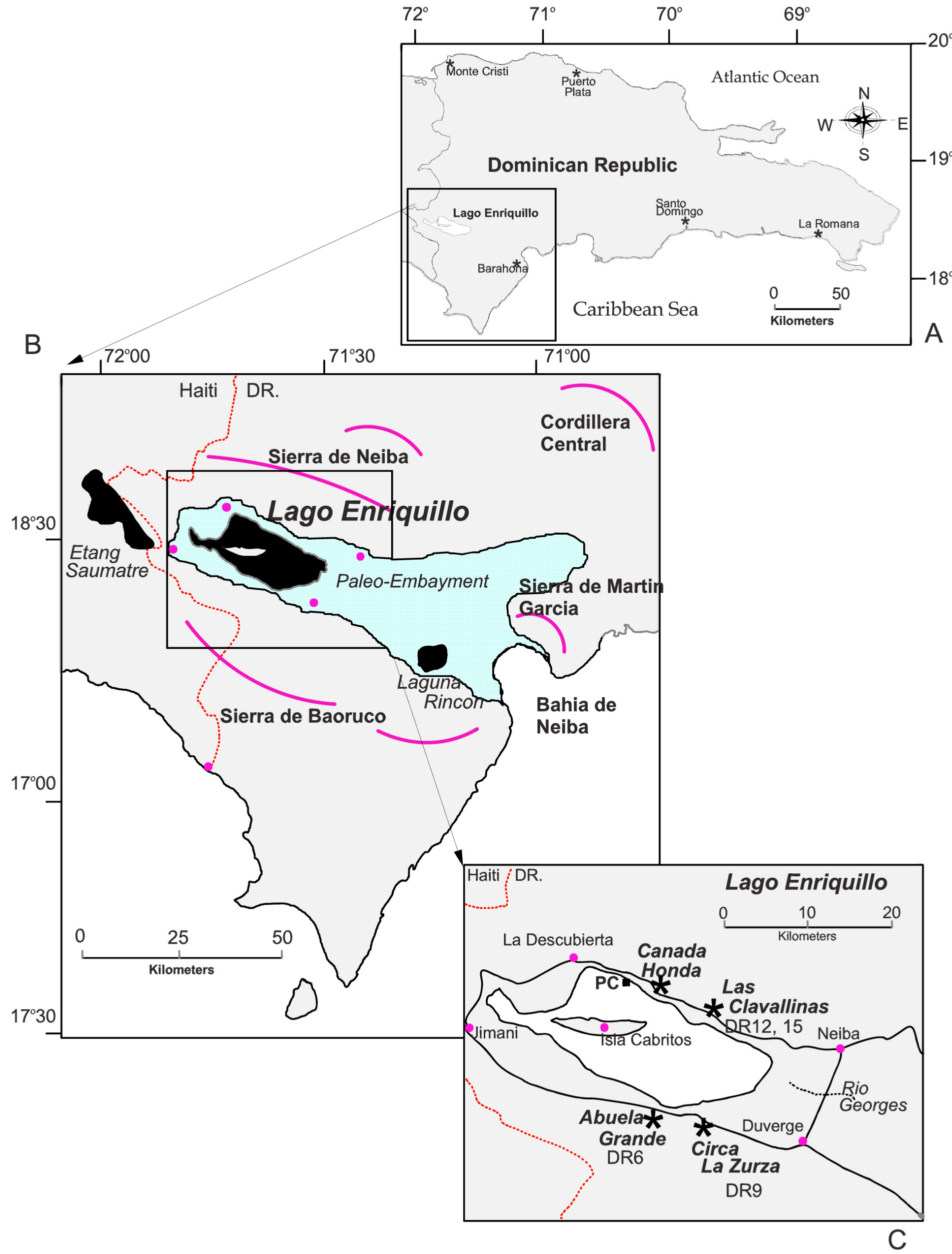

Figure 1. Location maps showing the (a) Dominican Republic and (b) Jaragua Peninsula. The Enriquillo Valley trends approximately NW to SE. Mountain chains are indicated by arcs concave toward drainage direction. The approximate location of the paleo-Enriquillo embayment is shaded. (c) Sample sites proximal to Lake Enriquillo. DR 9 was collected from Abuela Grande and DR 6 was collected from Circa La Zurza on the south shore of Lago Enriquillo. DR 12 and DR 15 were collected from Las Clavallinas, and Canada Honda marks the uppermost Holocene reef elevation. PC notes the location of Parque Cabritos, where water samples were collected. Rio Georges (dashed line) notes the channel reactivated after Hurricane Georges in 1998.

Republic to the Baie de Port-au-Prince in southeastern Haiti (Figure 1). Surrounded by mountains, Lake Enriquillo occupies the center of the valley, stretching from close to the Haitian border to ~30–35 km eastward (Figure 1). Lake Enriquillo, the largest saltwater lake in the Caribbean, lies in the western portion of the valley and covers ~300 km^2 of the valley floor. The Neiba and Baoruco Mountains, each with elevations higher than 2500 m above sea level, border the northern and southern shores of Lake Enriquillo. The lake became separated from the Caribbean by flood plain and alluvium deposits to the east of the valley between ~4.3 and 4.0 kyr [*Taylor et al.*, 1985; *Greer*, 2001]. Until that time it was in open communication with the Caribbean Sea. The water level of the lake now stands approximately 40 m

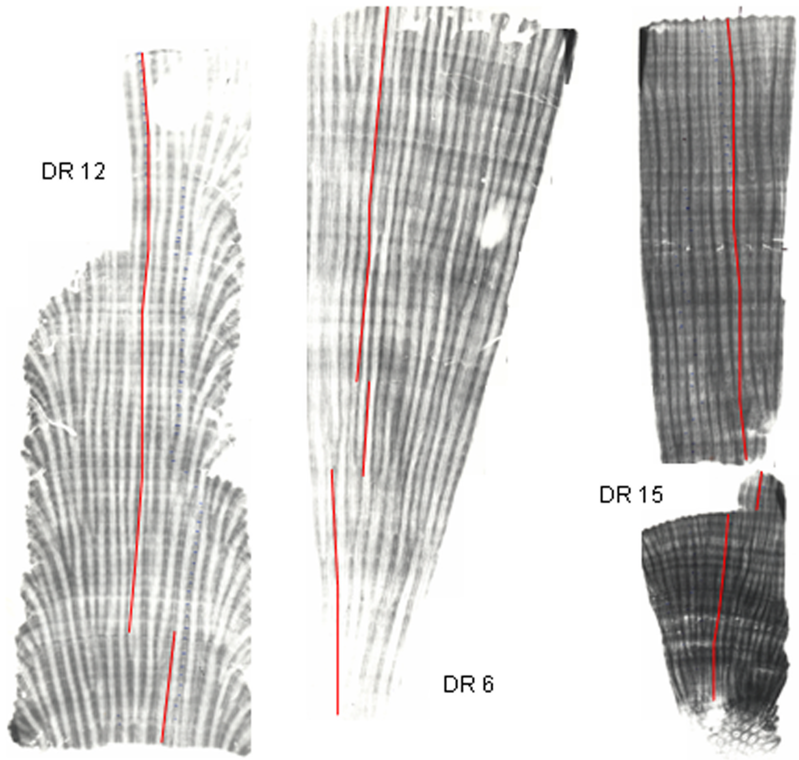

Figure 2. X radiographs of all sections of (left) DR 12, (middle) DR 6, and (right) DR 15. Breaks between coral sections were estimated and accounted for in the data. Approximate sample paths are indicated on each coral section. The entire length of DR 12 is ~19 cm, DR 6 is ~22 cm, and DR 15 is ~20 cm.

below sea level exposing a well-developed Holocene fringing reef and postreefal sedimentary deposits. The salinity of Lake Enriquillo is highly variable, ranging from 98 ppt (8 July 1998) to 44 ppt (26 November 2004) nearshore. Road cuts, gullies, out washes, and quarries along the lake have exposed thick sequences of Holocene corals in growth position. *Montastraea sp.* and *Siderastrea siderea* are most common. With some exceptions, the ecology, zonation, and diversity of reef deposits in the Enriquillo exposure are similar to that found in modern reefs throughout the Caribbean [*Stemann and Johnson*, 1992]. No major unconformities have been observed in Holocene reef strata.

[13] Exposed Holocene reef outcrops were located in gullies, road cuts, and abandoned quarries around the perimeter of the Enriquillo Valley floor (Figure 1). The pristine three-dimensional preservation of the reef outcrop allowed collection of consecutive sequences of corals. Corals reflecting over 1,000 years of combined growth with varying degrees of continuity were obtained. Both *Siderastrea sp*. and the *Montastraea annularis* species complex described by *Knowlton et al.* [1992] (*M. annularis*, *M. faveolata*, *M. franksii*) were collected. This study focuses on data from a specimen of *Montastraea annularis* (DR9) from Abuela Grande, two specimens of *Siderastrea sp.* corals (DR12 and DR15) from Arroyo Las Clavallinas, and one *Siderastrea sp.* coral from Circa La Zurza (Figure 1). Though rates of uplift have not been fully constrained at particular sites in the Enriquillo Valley [*Mann et al.*, 1995], uplift appears to be minimal at all sample locations and no evidence of folding or faulting of Holocene reef sediments was found in this study. Specimens DR15, DR12 and DR9 were collected at elevations of ~14.64, 13.44 and 15.57 m below present mean sea level and presumably grew at similar shallower depths. The exact elevation of DR6 could not be determined because of logistical constraints but is estimated to be within a similar depth range. Data presented here include 367 individual years of coral growth between ~7.2 and 5.3 kyr.

2.2. Sclerochronology

[14] All coral specimens were sliced with a diamond edged saw and x-rayed to illuminate density patterns. X-radiographs of all coral specimens are shown in Figures 2 and 3. Annual extension rates were assessed by measuring the maximum distance between adjacent dark carbonate bands. Total extension for each year was measured with calipers along the axis of maximum skeletal extension at a resolution of 0.1 mm. Mean annual extension rate data for each coral are reported in Table 1. Corals were then examined for fluorescent banding patterns using an automated pulsed nitrogen laser coupled with a fiber-optic bundle and a UV-enhanced photocell [*Milne and Swart*, 1994]. The content of detritus incorporated coral skeletal

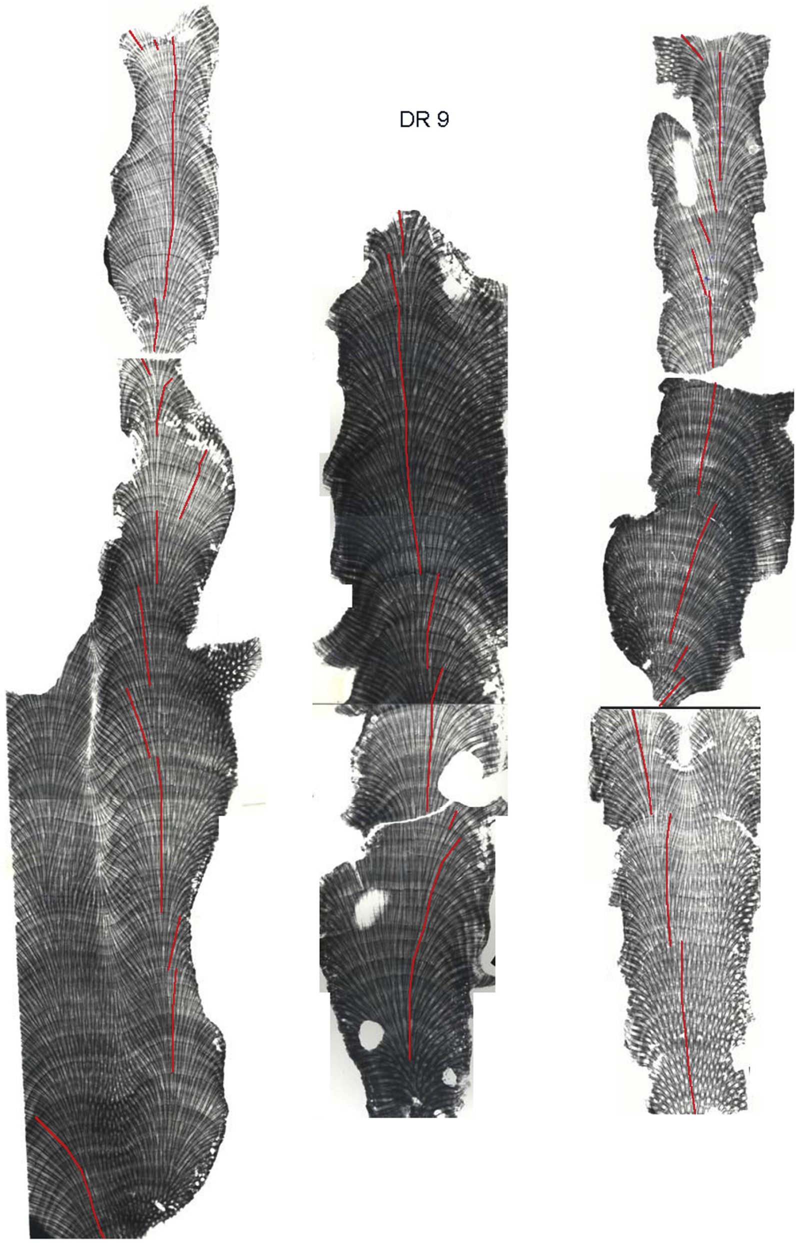

Figure 3. X-radiographs of all sections of DR 9 from left bottom (oldest) to right top (youngest). Breaks between coral sections were estimated and accounted for in the data. Approximate sample paths are indicated on each coral section. The entire length of DR9 is ~1.6 m.

framework was examined via scanning electron microscopy (SEM) with energy dispersive X-ray analysis.

2.3. Age Model for Corals

[15] All coral specimens were assessed for possible diagenetic alteration from aragonite to low-Mg calcite using standard X-ray diffraction techniques on a Scintag 2000 2-theta X-ray diffraction instrument. Select corals were prepared for ^{230}Th/^{234}U isotopic measurement via methods described by *Hamelein et al.* [1991]. Corals from the Enriquillo Valley range in age from 5297 ± 41 to 7203 ± 77 calendar years before present.

[16] It is believed that the densest portion of the annual coral growth couplet is formed in coincidence with the warmest seasonal SSTs [*Hudson*, 1981; *Lough and Barnes*, 1990], which presently occur during August and September in the Caribbean according to COADS data [*Slutz et al.*, 1985]. This time period corresponds with increased regional precipitation. Coincident increases in temperature and precipitation act to deplete δ^{18}O values of marine waters. Hence we have assigned the most negative δ^{18}O of Holocene coral skeletons to occur at the time of highest temperature and precipitation. Coral chronologies were initially based on the assignment of age according to density banding. As density-banding interpretation is quantitatively

Table 1. Age and Stable Isotopic Data

Coral Identification[a]	DR15	DR12	DR9	DR6
Location	Las Clavallinas	Las Clavallinas	Abuela Grande	Circa La Zurza
Elevation, m	−14.64	−12.44	−16.73	
Age, ka	7.203 (±77)	6.945 (±75)	6.037 (±−46) and 5.885 (±−87)	5.297 (±−41)
Mean annual extension, mm	3.36	3.00	8.06	4.63
Mean sample resolution, per year	6.1	5.5	4.0	8.0
N	60	63	197	47
Species	*Siderastrea sp.*	*Siderastrea sp.*	*Montastraea annularis*	*Siderastrea sp.*
Aragonite, %	100	98–100	100	100
Mean C	−4.46	−2.80	−3.34	−2.49
Minimum C	−6.03	−3.45	−4.77	−3.06
Maximum C	−3.48	−2.18	−2.33	−1.95
Range C	2.55	1.27	2.44	1.11
Mean O	−2.71	−3.13	−3.16	−2.70
Minimum O	−4.11	−4.20	−4.94	−3.61
Maximum O	−1.92	−2.50	−1.94	−2.10
Range O	2.18	1.70	3.0	1.51

[a]Elevations are reported relative to present mean sea level. Ages obtained from $^{230}Th/^{238}U$ analyses are reported with calculated error. Two dates were obtained from the ~200 continuous year coral DR9. *N* is number of years analyzed. Sample mineralogy, determined by X-ray diffraction methods, is expressed as percent aragonite. Mean, minimum, maximum, and range carbon and oxygen isotopic values are expressed in parts per million.

imprecise, chronologies were refined using the observed oxygen isotopic minima. Therefore coral 'years' begin in the warm/wet season and extend to the next season.

[17] In some corals, seasonal patterns in the $\delta^{13}C$ of coral carbonate were more reliable indicators of seasonal cycle than $\delta^{18}O$ patterns, providing a clearer high-amplitude annual fluctuation. Although the cause for this is unknown at present, the $\delta^{13}C$ minima of many corals lag the oxygen isotopic minima by approximately 2–3 months. Therefore when $\delta^{18}O$ records were unclear, ages were assigned using seasonal $\delta^{13}C$ patterns and corrected for a 2-month lag.

2.4. Stable Isotopic Analysis

[18] Powdered calcium carbonate was sampled from selected coral specimens using a computer controlled drilling apparatus with an attached diamond tipped drill bit. As a result of variations in growth between species and individual corals, corals were sampled at different resolutions. The sampling resolutions for corals used in this study are summarized in Table 1. Sampling resolution was held constant for each individual coral and all corals were sampled at a resolution of at least 4 samples per coral year, a resolution considered adequate to capture decadal patterns in isotopic composition [*Quinn et al.*, 1996], if not precise seasonal patterns. All specimens were drilled in continuous transect increments along the thecal wall of the coral skeleton, parallel to the axis of primary growth. *Swart and Leder* [1995] have shown that this sampling methodology does not affect the original carbon and oxygen isotopic composition of the coral skeleton.

[19] Carbonate powder samples were stored in copper boats in a desicator and analyzed using a Finnigan-MAT 251 mass spectrometer connected to an automated extraction device. Isotopic data are presented in standard delta notation relative to V-PDB and have been corrected for the usual isobaric interferences. Data reported herein are available electronically at the World Data Center-A for Paleoclimatology.

2.5. Time Series Analysis

[20] While data from each coral were examined qualitatively for cyclicity in variability, only DR 9 represents a length of continuous coral growth long enough (n = 197 years) to allow quantitative time series analysis of annual data. The following methods for time series analysis of DR 9 are based on protocol outlined by *Box et al.* [1994], *Koopmans* [1995], *Warner* [1998] and *Bloomfield* [2000]. In preparation for spectral analysis, missing values in data were approximated via linear interpolation of adjacent points and data were detrended (centered). Power spectra were calculated using a Daniell (equal weight) smoothing function with a 5 point window using SPSS TRENDS software (SPSS Inc., Chicago, Illinois). To test the statistical significance of apparent decadal- to multidecadal-scale peaks, 95% confidence intervals were calculated for spectral densities using a chi-square distribution. The equivalent degrees of freedom for spectral density data are calculated as 2M, where M is the width of the Daniell window (5). A peak may be considered significantly higher than expected by chance if the confidence intervals do not overlap mean spectral density of the series [*Koopmans*, 1995; *Warner*, 1998].

3. Results

3.1. Sclerochronology

[21] X-ray diffraction analyses showed that all specimens in this study (DR6, DR9, DR12, ands DR15) were composed of 98–100% aragonite (Table 1). Fluorescence and SEM analyses were performed to investigate possible freshwater influences on coral growth. Results of both examinations were inconclusive. While fluorescent bands were observed in some Holocene corals, banding patterns were indistinct and even absent in some specimens. Scanning electron microscopy revealed the presence of what may have been detrital sediment trapped within coral skeletal architecture (which could indicate storm sedimentation). However, all presumed detrital material consisted of carbonate, and could therefore not be reliably distinguished from in situ sediment that may have been created during sample cutting and processing.

3.2. Modern Regional Precipitation, Temperature, and Hurricane Data

[22] The Dominican Republic has been marked by the passage of several devastating hurricanes and tropical

storms in the last century. Limited quantitative data on hurricanes date back to the late fifteenth century and more detailed records of hurricanes over the last century are available [*Landsea*, 1993; *Neumann et al.*, 1993; C. Landsea, Colorado State Hurricane Database, available at http://weather.unisys.com/hurricane/atlantic/, maintained by the forecasters and researchers at the National Hurricane Center in Miami, Florida, based upon "A tropical cyclone data tape for the North Atlantic basin, 1886–1983: Contents, limitations, and uses," NOAA Technical Memorandum NWS NHC 22, 1984, written by B. R. Jarvinen, C. J. Neumann, and M. A. S. Davis, 1998 (last modified), hereinafter referred to as Landsea, Colorado State Hurricane Database, 1998]. Many of these storms have passed directly over sites chosen for this study. The impact of hurricanes on the geology and human populations of the country has been dramatic. Although there are no definitive data on storm frequency during the study period represented by the Enriquillo corals, some information may be inferred by examining regional tropical storm activity over the past 130 years. During this period 61 storms have passed within 200 km of the valley from 1870–2000 according to *Neumann et al.* [1993] and Landsea (Colorado State Hurricane Database, 1998). Thirty-three of these storms have been tropical storm or tropical depression status and 22 of these storms have been category 1 hurricanes or stronger.

[23] Regional precipitation data from the last two centuries were obtained from the NOAA NCDC website (Data are available from the World Wide Web server for NOAA Baseline Climatological Data set, Monthly Weather Station Temperature and Precipitation Data, available at http://ingrid.ldeo.columbia.edu/) cataloging monthly weather stations worldwide. Approximately 900 months of precipitation and temperature data measurements were recorded from 1888–1963 in Port-au-Prince, Haiti (Lamont IRI data, station 7843900). This station, located at 18.57°N, 72.30°W (31 m above sea level) was chosen as it contained the longest and most continuous record of both variables of all reported stations and is reasonably proximal to the Enriquillo Valley. Mean precipitation over the measurement period was 110.12 mm (SD = 85.10) and mean temperature was 26.50°C (SD = 1.27). Data concerning historical tropical storm occurrence, position, strength and duration were compiled primarily from *Landsea* [1993], *Neumann et al.* [1993] and Landsea (Colorado State Hurricane Database, 1998). Modern regional precipitation data were examined as a potential analog for Holocene rainfall. Port-au-Prince temperature data (not shown) suggest a periodicity of ~12–13 years but significance cannot be tested.

3.3. Stable Isotopic Data

[24] The raw $\delta^{18}O$ and $\delta^{13}C$ data from corals DR15, DR12, DR9, and DR6 are shown interpolated to monthly values in Figure 4. For illustrative purposes, the original raw data, smoothed by a 5-year running mean to filter out higher-frequency variability and highlight lower-frequency (decadal to multidecadal) variability, are shown in Figure 5.

[25] The records of $\delta^{18}O$ and $\delta^{13}C$ in DR6, DR12, and DR15 as well as recent precipitation data from Haiti are too short to assume any statistically significant decadal cyclicity in isotopic composition. However, qualitative inspection of these time series suggests that cyclic patterns may be present in the $\delta^{18}O$ and $\delta^{13}C$ of several corals and perhaps precipitation data. As significance of these potential patterns cannot be assessed statistically, a simulated sine wave of appropriate (estimated) frequency is plotted with most coral and precipitation data in Figure 6 for illustrative purposes (following *Warner* [1998]). Patterns in $\delta^{13}C$ and $\delta^{18}O$ of most corals in this study suggest oscillations on a roughly decadal to multidecadal scale (Figure 6), with an approximate frequency of 17–20 years for all corals. For DR15, the estimated 8-year hiatus at ~7235 years before present also makes recognition of statistically significant decadal patterns impossible for this coral. However, the $\delta^{18}O$ and $\delta^{13}C$ records shown in Figure 6 indicate a potentially strong decadal to multidecadal signal, particularly in $\delta^{13}C$ in this coral. A sine wave with a period of 15–16 years is superimposed on modern Port-au-Prince precipitation data to illustrate a possible 15-year periodicity where each trough in the sine wave is accompanied by an increase in precipitation (Figure 6).

[26] The statistical significance of these apparent cycles can only be assessed for DR 9 (n = 197). The decadal fluctuations in $\delta^{13}C$ of DR 9 are particularly dramatic from ~6000 to 5940 years and 5895 to 5875 years before present (Figure 6). Results of spectral analyses (Figure 7) indicate significant, broad spectral peaks in both $\delta^{13}C$ and $\delta^{18}O$ of DR9 at ~15 and 20 year periods (respectively).

4. Discussion

[27] The 15- to 20-year cycle in coral isotopic data is most clearly suggested in Figure 6. We propose that local temperature, while potentially a contributor to variations in the oxygen isotopic composition, is not likely to be the primary driver of these decadal to multidecadal oscillations. The rationale for attributing variability primarily to precipitation and the potential sources for precipitation-dominated fluctuations in the isotopic composition of paleo-Enriquillo water are discussed below.

4.1. Temperature Versus Precipitation (Salinity)

[28] The range in $\delta^{18}O$ for each Enriquillo coral can be converted to temperature using a known calibration between $\delta^{18}O$ and temperature [*Leder et al.*, 1996] via the equation below if we hold δw constant (therefore assuming all variability to be temperature dependant):

$$T^{\circ}C = 5.33 - 4.519(\pm 0.19) * (\delta c - \delta w)$$

[29] Using this equation, the calculated temperature range for corals in this study (up to ~12.7°C for raw annual data) is inconsistent with historical temperature changes in the region. While SST data from the last century certainly cannot serve as an exact analog for mid-Holocene temperatures, there is no evidence in the literature for Holocene SST ranges that were different by the orders of magnitude that would explain the isotopic data in Enriquillo corals. Reynolds and COADS SST data and temperature data from Port-au-Prince all indicate a maximum mean annual SST

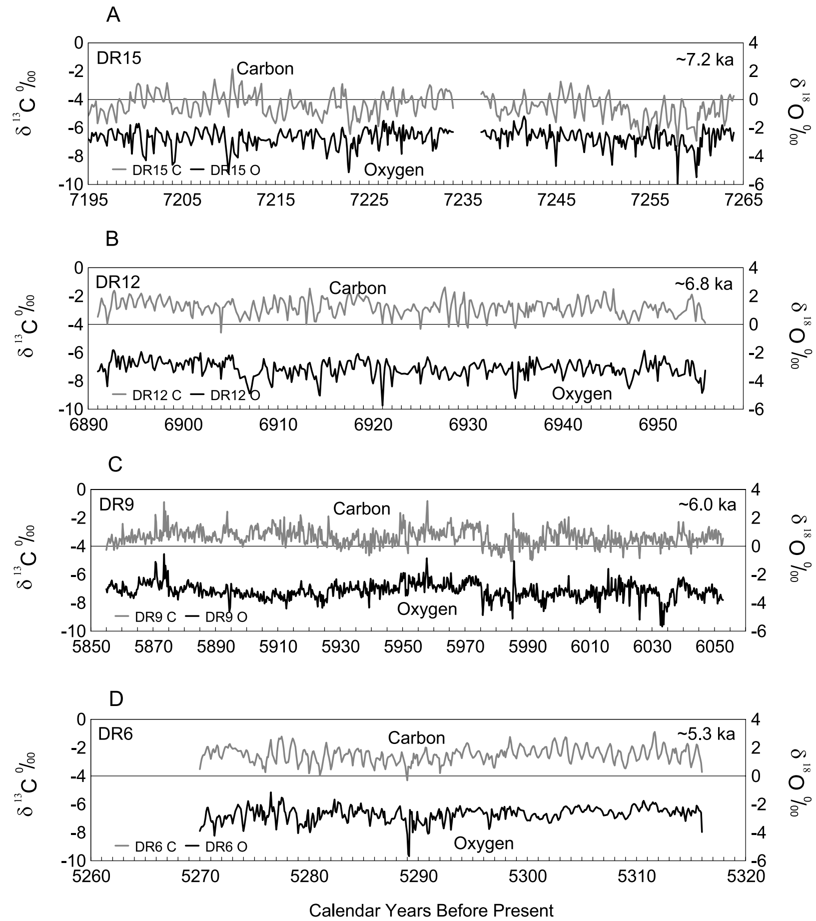

Figure 4. Monthly interpolated carbon and oxygen isotopic data from corals (a) DR15, (b) DR12, (c) DR9, and (d) DR6. DR6, DR12, and DR15 are *Siderastrea sp*. corals. DR9 is a *Montastraea annularis* coral. Note that the *x* scale (time) differs for each coral.

range of less than 2°C in the last century offshore of the Jaragua Peninsula. The annual range in δ^{18}O of the Holocene *Siderastrea sp*. corals are approximately equal to the −1.5‰ range in δ^{18}O of a modern coral from the southeastern Dominican Republic [*Greer*, 2001]. However, the total δ^{18}O range of the *Montastraea annularis* coral (DR9) is approximately twice that of the Holocene *Siderastrea sp.* specimens. This could be a result of slightly different sampling resolution in that the growth rate of *Siderastrea sp.* is lower than *Montastraea sp*. If the range in δ^{18}O was primarily controlled by temperature, the 6 kyr record theoretically represents a temperature range of ∼7°C (mean annual value) to 12.7°C (raw annual value). There is no existing evidence to indicate decadal changes in Holocene normal marine sea surface temperature of this scale.

[30] There is also no theoretical evidence for such ranges in temperature in the paleo-Enriquillo embayment. While it is possible that temperature fluctuations in the paleo-Enriquillo embayment were greater than at present, a 7°–13°C range in mean annual temperature at 6 ka is highly unlikely. During the mid-Holocene, the embayment was more extensive and far greater in depth. As the lake occupies a basin that has presumably undergone infilling since closure, the elevation of the lake bottom has most likely continued to increase throughout the Holocene. Coral DR9 grew at an estimated depth of between 16.73 m below present sea level (base of coral) and 14.41 m below present mean sea level (top of coral) when the mean depth of Lake Enriquillo was far greater (by perhaps up to 30 m). At that time, the embayment was in full communication with the Caribbean Sea.

[31] A second indication that temperature is not the sole driver of stable isotopic variability in the geochemistry of these coral skeletons is the covariance of δ^{13}C and δ^{18}O for all corals in this study. The positive correlation between mean annual δ^{13}C and δ^{18}O and the similar decadal-scale patterns in geochemical variability of all Holocene corals provides indirect evidence that temperature was not the main factor controlling coral δ^{18}O. While temperature can influence the δ^{18}O of corals, temperature is not a direct control on coral δ^{13}C [*Emrich et al.*, 1970]. Therefore the positive correlation between δ^{13}C and δ^{18}O on a multidecadal timescale indicates that factors other than temperature are probably responsible. While it is possible for other variables known to control coral δ^{13}C (such as solar insolation) to covary with temperature on a seasonal scale [*Grottoli*, 2001], there is no evidence for covariance on the decadal scale represented by corals in this study. Further-

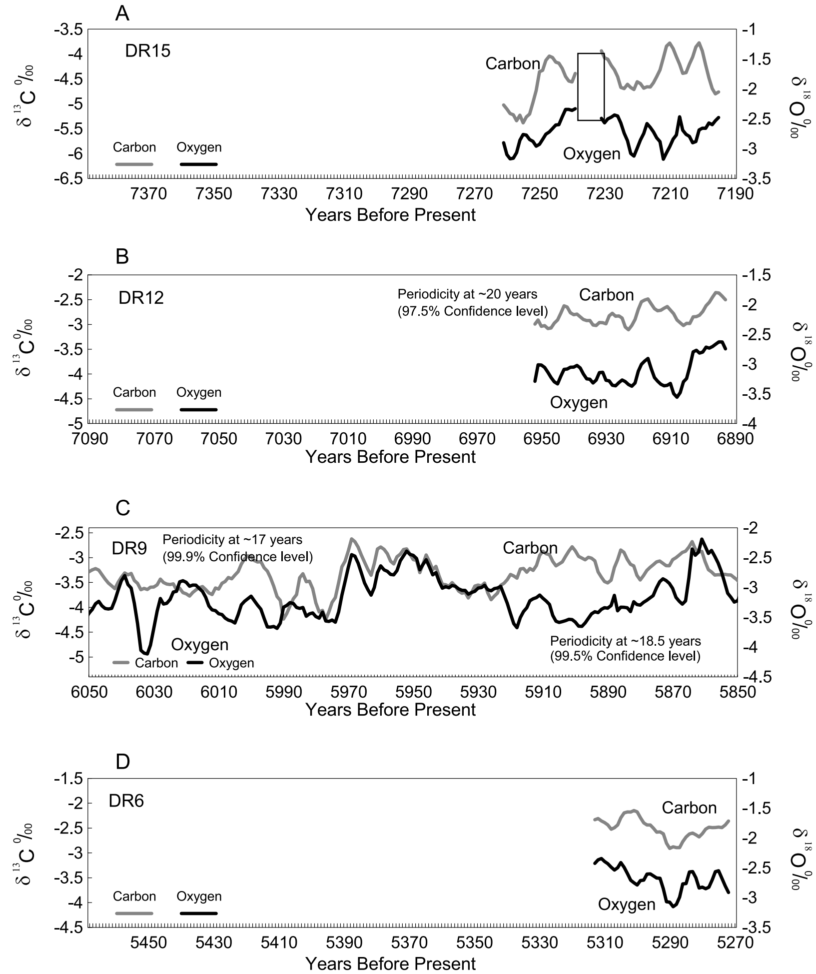

Figure 5. Interpolated annual oxygen isotopic variations for (a) DR15 (7.2 ka), (b) DR12 (6.8 ka), (c) DR9 (6.0 ka), and (d) DR6 (5.2 ka) with a 5-year smoothing function applied to factor out high-frequency or random noise. The rectangle in Figure 5a indicates a hiatus in data acquisition.

more, the decadal-scale patterns exhibited by corals in this study cannot be explained by known frequencies of solar variability reported in the literature (e.g., the 11-year sunspot cycle) although some records are too short to entirely rule out a solar component to all isotopic variability. The high extension rate and continuous growth of corals such as DR9 are not typical of growth in a highly variable or stressed temperature regime and evidence of stress banding [*Hudson et al.*, 1976] is virtually absent from the corals examined for stable isotopic composition. Detailed analyses of independent temperature proxies (i.e., minor elements) would better eliminate temperature as the primary driver for stable isotopic variability in these corals.

4.2. Precipitation (Salinity)/$\delta^{18}O$ Relationship

[32] In addition to temperature, the $\delta^{18}O$ of coral skeleton is influenced by the $\delta^{18}O$ composition of surrounding water, which in turn is controlled by the amount of local evaporation and input of isotopically light freshwater. As tropical temperature variations are minimal on decadal to interdecadal scales [*Enfield and Mayer*, 1997], the $\delta^{18}O$ of the coral skeleton may disproportionably reflect salinity fluctuations, particularly during extreme precipitation events. Precipitation and flooding effects are amplified in mountainous regions such as the Enriquillo Valley where orographic isotopic depletion effects [*Poage and Chamberlain*, 2001; *Stern and Blisniuk*, 2002] are more pronounced.

[33] Although coral $\delta^{18}O$ records have been successfully correlated with regional precipitation anomalies [*Cole and Fairbanks*, 1990; *Cole et al.*, 1993; *Swart et al.*, 1996b], the complex nature of most regional hydrologic environments makes a direct correlation between $\delta^{18}O$ and absolute salinity difficult. *Cole et al.* [1993] examined the relationship between proxy $\delta^{18}O$ and ENSO variability. However, in addition to a simple Rayleigh Distillation model (precipitation and evaporation), orographic and inland effects as well as the mixing of various water masses may complicate any initial linear agreement between $\delta^{18}O$ and salinity.

[34] There have been some attempts to collect data on the observed relationship between $\delta^{18}O$ of water and salinity [*Swart et al.*, 2003; *Watanabe et al.*, 2002; *Fairbanks*, 1982] in the Atlantic Ocean. These studies show that the relationship between $\delta^{18}O$ and salinity may vary locally or regionally because of a number of isotopic (e.g., orographic and

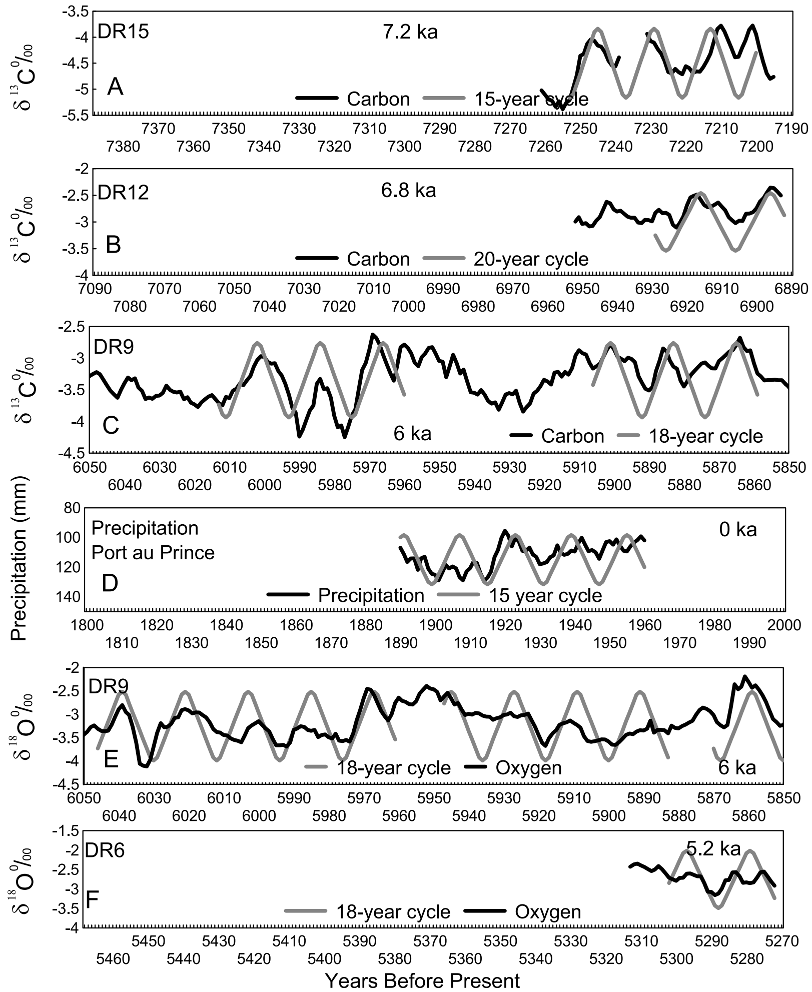

Figure 6. The 14- to 20-year cycles suggested by oxygen and carbon isotopic variations of several corals in this study. Interpolated annual carbon isotopic variations for (a) DR15, (b) DR12, and (c) DR9 with (d) modern Port-au-Prince precipitation data and annual oxygen isotopic variations for (e) DR9 and (f) DR6. All data have a 5-year smoothing function applied to factor out high-frequency noise. A 15- to 16-year sine wave is superimposed on data in Figure 6a; a 17- to 18-year sine wave is superimposed on data in Figures 6c, 6e and 6f; and a 19- to 20-year sine wave is superimposed on data in Figure 6b to illustrate the dominant periodicities suggested by qualitative analysis or indicated by time series analysis. A 15- to 16-year sine wave is superimposed on precipitation data (Figure 6d) to illustrate a similar possible cycle in modern precipitation.

latitude effects) and oceanographic phenomena (mixing of water masses, precipitation and ocean circulation patterns). *Fairbanks* [1982] reported that along the eastern seaboard (from Nova Scotia to Cape Hatteras) a change of one salinity unit (ppt) translates to a change in δ^{18}O of between ~0.6‰ and ~0.3‰. *Swart et al.* [2003] has measured the δ^{18}O/salinity relationship for water in the Caribbean Antilles as ~0.2‰ isotopic change per salinity unit. It is likely that in closed basins the relationship can be even more extreme and varied [*Swart et al.*, 1996a, 2001].

[35] Instrumental salinity data proximal to the island of Hispaniola are incomplete at best. The seasonal range in mean salinity is ~1 ppt at 0–10 m depth at present (Salinity from World Ocean Atlas 2001(WOA 01) for 1° × 1° centered at 17.5°N, 70.5° W, available at http://iridl.ldeo.columbia.edu/SOURCES/.NOAA/NODC/WOA01/dataset_documentation.html, 2001). While salinity currently varies on very short (seasonal) timescales, there is no evidence that the salinity of greater Caribbean seawater as controlled by conditions in the Atlantic ocean fluctuates greatly on decadal timescales at present [*Swart et al.*, 2003]. If this is true for the Holocene, and the temperature effect is assumed to be zero (simulating maximum salinity related effects on δ^{18}O), estimates of the maximum salinity change allowed for by the Holocene δ^{18}O (a range of ~1.5 to 3.0‰) coincide with a change of 2–3 ppt to 15 ppt [*Fairbanks*, 1982; *Swart et al.*, 1999; *Swart et al.*, 2003] in the paleo-Enriquillo Valley. While a shift of 15 ppt is dramatic, it is possible for certain species to survive comparable variable salinities, if not for sustained periods [*Swart et al.*, 2001]. While a change in salinity of 15 ppt may affect coral extension rate it will not necessarily result

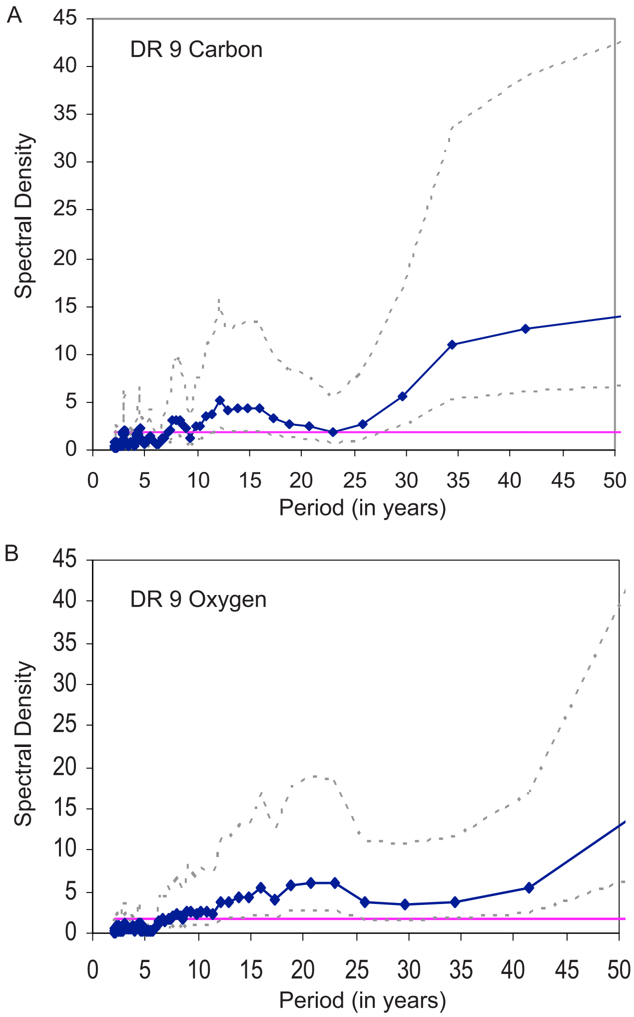

Figure 7. Spectral analyses of (a) mean annual carbon and (b) oxygen isotopic data for DR 9. Spectral density (points interpolated by solid line) and 95% confidence intervals (dashed lines) are plotted in each graph. Mean spectral density of each series is indicated by a solid, horizontal line.

in a dramatic cessation of growth or sustained detrimental growth effects [*Swart et al.*, 1999; *Swart et al.*, 2001]. *Siderastrea sp*. corals are particularly known to thrive in highly variable salinity regimes [*Muthiga and Szmant*, 1987; *Swart et al.*, 2001].

4.3. Potential Sources for Regional Decadal Precipitation Anomalies

[36] There are currently three main sources for tropical precipitation in Hispaniola: convection, cyclonic activity (tropical storms and hurricanes), and orographic effects [*Hastenrath*, 1991]. It is possible that a more northerly path of ITCZ migration during mid-Holocene warming could have also served as an important driver of precipitation at this site in the past.

4.3.1. Patterns and Changes in ITCZ Migration Throughout the Holocene

[37] The tropical North Atlantic climate is primarily controlled by changes in the strength of trade winds, SST anomalies, and the position of the intertropical convergence zone (ITCZ) [*Hastenrath and Lamb*, 1977; *Peterson et al.*, 1991; *Black et al.*, 1999, 2004] which may be governed by insolation [*Poore et al.*, 2004]. When the tropical North Atlantic is cool relative to the tropical South Atlantic, increased surface pressure in the north forces the ITCZ to move south [*Hastenrath and Greischar*, 1993; *Carton et al.*, 1996]. Therefore in the Northern Hemisphere winter the prevailing northeast trade winds push the ITCZ south, while in the summer southeast trade winds force the ITCZ to migrate north. Changes in seasonal insolation mediate trade wind strength [*Braconnot et al.*, 2000], and precede changes in SST anomalies [*Nobre and Shukla*, 1996]. Under present conditions the ITCZ is farthest north in August and September and closest to the equator in March and April [*Philander and Pacanowski*, 1986; *Black et al.*, 1999].

[38] As the ITCZ moves north into the Caribbean basin, precipitation may decrease the mean salinity of the southern Caribbean, and as the ITCZ moves south, precipitation decreases in the Caribbean and increases closer to the equator [*Black et al.*, 1999]. The migration of the ITCZ over the Atlantic roughly follows the solar cycle with a 2-month lag because of the slow surface heating of the ocean [*Braconnot et al.*, 2000]. The Greater Antilles are rarely under the direct influence of the ITCZ at present.

[39] Numerous theoretical, proxy [*Martin et al.*, 1997; *Haug et al.*, 2001; *Luckge et al.*, 2001; *Poore et al.*, 2003; *Tedesco and Thunell*, 2003; *Koutavas and Lynch-Stieglitz*, 2003; *Black et al.*, 2004], and model-based studies [*Prentice and Jolly*, 2000] indicate that the Northern Hemisphere seasonal cycle was intensified during the mid-Holocene because of increased seasonal insolation [*Berger*, 1978; *Kutzbach*, 1981] and that the ITCZ migrated farther north in the mid-Holocene. During the early Holocene, increased insolation in the northern summer contributed to increasingly warm humid conditions in the tropics [*Stager and Mayewski*, 1997; *Crowley and North*, 1991]. Using orbital parameters for 6 ka derived from *Berger* [1978], *Braconnot et al.* [2000] compared models of coupled ocean-atmosphere dynamics and constant SST to look at the role of ocean circulation in governing 6 ka climate. The *Braconnot et al.* [2000] model shows enhanced equatorial heating and an increased seasonal extent of the ITCZ at 6 ka forced by increased mid-Holocene insolation. The increased reach of the ITCZ resulted in greater transport of latent heat to higher latitudes via precipitation over the ocean.

[40] While precipitation anomalies currently associated with the ITCZ rarely impact the Greater Antilles directly at present, the *Braconnot et al.* [2000] model suggests an increase in precipitation over the Dominican Republic during the mid-Holocene summer as the ITCZ traveled farther north. A decadal-scale fluctuation in tropical Atlantic SSTs similar to documented variability at present [*Carton et al.*, 1996; *Chang et al.*, 1997; *Moron et al.*, 1998; *Hakkinen*, 2000; *Joyce et al.*, 2000; *Marshall et al.*, 2001; *Cobb et al.*, 2001] could have driven a similar decadal-scale migration of the ITCZ over Hispaniola. When northern tropical Atlantic temperatures were highest, the ITCZ migrated farther north over Hispaniola, resulting in a stronger precipitation anomaly at the study site. When

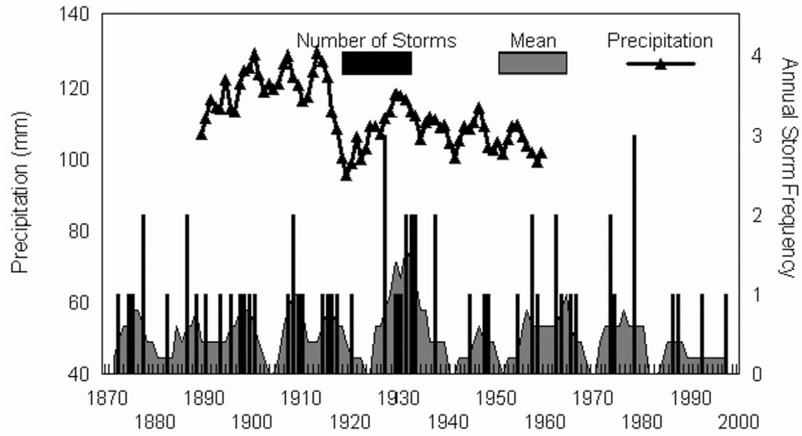

Figure 8. Tropical storm occurrence and precipitation data for the Enriquillo Valley region. Precipitation data from Haiti were obtained from the World Wide Web server for NOAA Baseline Climatological data set (monthly weather station temperature and precipitation data, available at http://ingrid.ldeo.columbia.edu/). Modern tropical storm and hurricane occurrence data (annual number of storms within 200 km of the Enriquillo Valley) were compiled from *Landsea* [1993], *Neumann et al.* [1993], and Landsea (Colorado State Hurricane Database, 1998).

cooler tropical North Atlantic SSTs prevailed the ITCZ exerted less influence over Enriquillo precipitation. With this scenario, decadal to multidecadal oscillations in Enriquillo coral δ^{18}O during the mid-Holocene may reflect insolation-related changes in thermal seasonality and/or changes in the position of the Atlantic Intertropical Convergence Zone.

4.3.2. Patterns in Storm Activity Throughout the Holocene

[41] Decadal and interdecadal patterns in hurricane activity have been recognized over historical timescales [*Landsea et al.*, 1992; *Zhang et al.*, 2000; *Elsner et al.*, 2000]. Several studies have noted an increase in tropical Atlantic storm frequency from the 1940s to the 1960s (~1944–1967) followed by a subsequent decline in activity (1968–1991) [*Mather et al.*, 1964; *Gray et al.*, 1997; *Zhang et al.*, 2000; *Elsner et al.*, 2000]. These periods have been characterized as active or passive hurricane phases. Multidecadal variability on this scale is most clearly observed in the record of intense hurricanes (Category 3, 4, 5) [*Landsea et al.*, 1996]. Patterns in tropical storm activity from historical records exist for the Enriquillo Valley region [*Landsea*, 1993; *Neumann et al.*, 1993; Landsea, Colorado State Hurricane Database, 1998] with an apparent period of ~15–18 years (Figure 8).

[42] In order to determine possible first-order mechanisms driving hurricane cyclicity, teleconnections between hurricane formation and other known climatic phenomena must be considered. Several key studies have determined that tropical Atlantic SST patterns, ENSO activity and precipitation patterns in the western African Sahel correlate with Atlantic hurricane activity [*Gray*, 1984b; *Landsea and Gray*, 1992; *Landsea et al.*, 1994; *Lighthill et al.*, 1994; *Landsea et al.*, 1996; *Gray et al.*, 1997; *Xie et al.*, 2002] and that each of these climatic phenomena are connected and operate on decadal to multidecadal timescales [*Molinari and Mestas-Nuñez*, 2003; *Giannini et al.*, 2004; *Kayano and Andreoli*, 2004; *Paeth and Hense*, 2004; *Labat et al.*, 2004].

[43] During El Niño events, increased vertical wind shear over the tropical Atlantic results in a decrease in Atlantic hurricane activity [see *Gray*, 1984a; *Gray et al.*, 1997]. A particularly critical area for the formation and continuation of hurricanes lies immediately east of the Antilles [*Gray*, 1984b; *Gray et al.*, 1997]. If westerly winds are strong in this region, the probability of hurricane formation can decrease dramatically. Therefore few hurricanes cross the Caribbean in El Nino years [*Gray et al.*, 1997]. It has been suggested, using evidence from a tropical coupled ocean atmosphere model, that changes in the strength and timing of ENSO activity during the Holocene may have even indirectly impacted thermohaline circulation during the Younger Dryas [*Clement et al.*, 2001]. It is also possible that the combined cyclicity of ENSO variability, tropical Atlantic SST fluctuations, and the corresponding patterns in Sahel precipitation that produce decadal patterns in hurricane frequency are ultimately driven by patterns in thermohaline circulation. During years of increased thermohaline strength (e.g., 1924–1939 and 1950–1964), wet conditions existed in the African Sahel, ENSO frequency and intensity was low, and Atlantic hurricane activity increased. Each of the periods of coherent ENSO, Sahel, hurricane and thermohaline characteristics described by *Gray et al.* [1997] lasted for ~14 or 15 years, which is approximately consistent in frequency with δ^{18}O and δ^{13}C data from the present study as well as modern Caribbean storm frequency data (Figure 8).

[44] Variations in precipitation in the Enriquillo Valley at present may be driven by a number of sources, but the most dramatic precipitation anomalies occur as a consequence of passing tropical storms and hurricanes. In the last century,

mean annual precipitation during all but four years experiencing the passage of hurricanes was 19 cm above average according to modern hurricane data and precipitation data from Haiti. The modern relationship between precipitation and hurricane occurrence for the region is shown in Figure 8.

[45] In addition to the temporary precipitation anomalies expected to accompany hurricanes in this region, sustained changes in regional geomorphology and hydrology result from the passage of storms in this region. Direct evidence of the effects of regional hurricane activity was observed in October 1998, one month after the passage of Hurricane Georges. The effects of Hurricane Georges were profound and severe flooding associated with the storm cut off access to the western third of the country for over a week. The Rio Yaque del Sur swelled with torrential rains, jumped its banks and spread into the town of Tamayo, located east of Lake Enriquillo in the Enriquillo Valley. Tamayo and nearby Jaquimeyes were submerged in up to 2 m of water and the river was more than a kilometer wide for weeks at this site.

[46] Mean annual precipitation in the valley is ∼90 cm (only 2% of which is estimated to reach the lake because of intense evaporation) and the lake is currently well mixed to a depth of at least 5 m [*Schubert*, 2000]. According to *Schubert* [2000], the Rio Yaque del Sur received up to 700 mm of precipitation in one night during the passage of Hurricane Georges. As a consequence of hurricane related precipitation and flooding, a previously dry channel (observed dry from May 1996 to June 1998) at the neck of the Enriquillo Valley was reactivated and began flowing west into Lake Enriquillo. The primary source of flow is either as a direct tributary of the Rio Yaque del Sur or from Laguna Rincon (Figure 1) into which the Rio Yaque del Sur flows.

[47] The reactivation of Rio Georges was accompanied by a dramatic rise in lake level. In the first month following Hurricane Georges, the lake level rose by over 1.5 m after which the lake level continued to rise because of the newly activated channel flow. The inundation of freshwater associated with Hurricane Georges and the reopening of this freshwater pathway dramatically altered the salinity of the lake from 98 ppt (8 July 1998) to 55 ppt (22 October 1998). *Schubert* [2000] estimated that the influx of freshwater to Lake Enriquillo as a consequence of Hurricane Georges was ∼1/4 of the influx associated with Hurricane David and Hurricane Frederic in 1979. The flow of freshwater into the valley via Rio Georges decreased after October 1998, but water still flowed west into the lake. As of June 2005 minimal freshwater still flowed into Lago Enriquillo via Rio Georges but a progressive restriction via alluvial sedimentation is clearly taking place. The mean salinity of nearshore Lago Enriquillo water was ∼90 ppt at that time and the lake level was clearly down based on previous observations. We propose that hurricanes had similar affects of the hydrology of the Enriquillo Valley during the mid-Holocene. When hurricanes altered the course of the Rio Yaque del Sur, a sustained multiyear influx of isotopically depleted water resulted.

[48] Therefore a decadal to multidecadal mode of tropical storm variability could have resulted in changes to the geomorphology of the Enriquillo embayment of the same temporal scale during the mid-Holocene. Variability in δ^{18}O (as a proxy for salinity) and δ^{13}C (as a proxy for terrestrial runoff) could be interpreted here as proxy indicators of mid-Holocene storm activity. Oscillations in δ^{18}O within the 15- to 20-year bandwidth may be interpreted to reflect alternating periods of high (low) precipitation that result in dramatic changes in the hydrology of the paleo-Enriquillo embayment. These changes in turn resulted in the sustained multiyear influx of isotopically depleted freshwater to the embayment, with highly evaporative conditions during years without storm activity. Similar decadal variations in the δ^{13}C of coral carbonate may reflect changes in the influx of hurricane-related organic matter to the marine environment. If so, the decadal to multidecadal patterns in isotropic variation of the Enriquillo corals (i.e., storm frequency) may ultimately be driven by SST anomalies in the greater tropical Atlantic. A link between tropical and subtropical SSTs and hurricane frequency in the Atlantic at present has been explored [*McCartney*, 1997; *Sutton and Allen*, 1997; *Molinari and Mestas-Nuñez*, 2003] and discrete SST anomalies on the scale of 12–14 years have been recognized in the tropical Atlantic [*Xie and Tanimoto*, 1998; *Tanimoto and Xie*, 1999; *Hakkinen*, 2000; *Chang et al.*, 2000].

[49] Deviations in the cyclic variation of stable isotopic composition related to precipitation and hurricane frequency are certainly expected. First, there is certainly a significant stochastic component to hurricane formation and path. To date hurricane forecasts remain uncertain even days in advance of passage over any given point. Secondly, the amount of precipitation associated with a passing hurricane depends on several factors including hurricane intensity, speed of passage, and path. Slow moving tropical storms may shed more precipitation than faster moving hurricanes. Thus there is no linear correlation between storm category and amount of rainfall. However, a relationship between precipitation and storm activity in general does exist. There is a clear increase in annual cumulative precipitation during most years of storm activity.

4.3.3. Variability in Holocene Orinoco and Amazon Outflow

[50] Patches of low-salinity water have been observed as far as 2000 km away from the Orinoco and Amazon Rivers via satellite observations [*Hu et al.*, 2004] and phytoplankton blooms thought to be related to Amazon and Orinoco outflow have been observed in the western tropical Atlantic [*Muller-Karger et al.*, 1995]. Correlations between the outflow of these rivers and local sea surface salinity have been observed as far north as Barbados [*Hellweger and Gordon*, 2002]. In addition, instrumental measurement of surface water δ^{18}O and salinity off Puerto Rico show dramatic fluctuations [*Watanabe et al.*, 2002] thought to be related to Orinoco outflow patterns. Previous workers have shown that there is also evidence of fluctuations in silicate off Puerto Rico that could be related to rainfall over the Orinoco River basin with a 3–4 month lag [*Froelich*, 1978; *Corredor and Morell*, 2001], suggesting a plausible link between Orinoco outflow and salinity in this region. It is therefore possible that fluctuations in Orinoco outflow could have influenced salinity throughout portions of the Caribbean during the Holocene.

[51] However no evidence suggests that a coherent Orinoco salinity signal has propagated as far as central or western Hispaniola in recent times. While a correlation between South American river outflow and salinity was observed or inferred in the eastern Caribbean [*Corredor and Morell*, 2001; *Hellweger and Gordon*, 2002], the correlation weakens considerably in the Central Caribbean, particularly at shallower depths because of dilution, mixing, evaporation, and precipitation processes [*Hellweger and Gordon*, 2002]. In addition, the changes in silicate content observed by *Froelich* [1978] were not accompanied by the larger variations in salinity observed by *Watanabe et al.* [2002].

[52] Analyses of the stable isotopic composition of skeletons around the island of Tobago, a locality considerably closer to the outflow of the Orinoco, showed little correlation between $\delta^{18}O$ and discharge [*Moses and Swart*, 2006]. A similar finding was observed between the Orinoco flow and the $\delta^{18}O$ of a modern coral sampled off the southeastern tip of Hispaniola just across the Mona Passage from Puerto Rico [*Greer*, 2001].

5. Conclusions

[53] Decadal to multidecadal (15–20 year) variations in regional Caribbean climate appear to be recorded in the $\delta^{13}C$ and $\delta^{18}O$ composition of Holocene corals from the Enriquillo Valley. Although temperature can better be eliminated as a primary driver of isotopic cyclicity with confirmation via independent proxy data (such as Sr/Ca), the magnitude of $\delta^{18}O$ isotopic variability in Enriquillo corals indicate a temperature range that is unrealistic for the mid-Holocene. Therefore data presented in this study suggest that while temperature fluctuations may contribute to the decadal to multidecadal mode of stable isotopic variability, local precipitation and/or fresh water flooding patterns are a more likely primary driver of $\delta^{13}C$ and $\delta^{18}O$ of Holocene coral skeletons from the Enriquillo Valley. These decadal-scale oscillations are interpreted to reflect regional precipitation patterns as influenced by the mid-Holocene migration of the ITCZ or precipitation and freshwater flooding patterns as driven by mid-Holocene hurricanes and tropical storms. Both hypotheses rely on a decadal to multidecadal mode of tropical Atlantic SST variability similar to that at present where SST anomalies have profound affects on global and regional atmospheric circulation that in turn affect Atlantic hurricane activity, West African (Sahel) drought and Pacific ENSO activity [*Gray et al.*, 1997]. Increased northern insolation during the mid-Holocene may have extended the influence of tropical SST anomalies to Hispaniola via a more northerly migration of the ITCZ on decadal to multidecadal timescales.

[54] There is abundant discussion in the scientific literature about whether global warming is contributing to an increase in the strength or number of tropical Atlantic storms [*Goldenberg et al.*, 2001; *Emanuel*, 2005; *Landsea*, 2005; *Pielke*, 2005; *Trenberth*, 2005; *Webster et al.*, 2005]. A reconstruction of mid-Holocene (6 ka) storm activity could provide a way to test this hypothesis. Preinstrumental records of tropical storm activity must be reconstructed via proxy records of paleoclimate variables to elucidate natural storm variability with changing boundary conditions. The persistence of a strong decadal mode of SST operation for a sustained period of time (2000 years during the mid-Holocene to present) would indicate that mechanisms for tropical Atlantic climate variability may not have changed significantly with time. This might have implications for the debate on whether human activities (e.g., the anthropogenic enhanced greenhouse effect) are currently affecting tropical storm dynamics. However, it may be possible that the frequency of these decadal-scale oscillations has increased slightly in this region from the mid-Holocene to present. Spectral data of the $\delta^{13}C$ and $\delta^{18}O$ of DR 9 peak between $\sim$15–20 years in contrast to the dominant 12–15 year mode of SST variability at present. The determination of a statistically significant change in frequency is beyond the scope of these data.

[55] **Acknowledgments.** We thank Amel Saied and Jim Rubenstone for laboratory assistance, and we greatly appreciate the generous use of Rick Fairbanks laboratory for coral age determination. We also wish to thank Robert Humston for expert insight and advice pertaining to statistical analysis of our data. Three anonymous reviewers provided valuable suggestions that greatly improved this manuscript. Funding for this research was provided by the Geological Society of America, the Miami Geological Society, Sigma Xi, and the American Association for Petroleum Geologists student grants in aid of research.

References

Beck, J. W., R. L. Edwards, E. Ito, F. W. Taylor, J. Recy, F. Rougerie, P. Joannot, and C. Henin (1992), Sea surface temperature from coral skeletal strontium/calcium ratios, *Science*, *257*, 644–647.

Berger, A. (1978), Long-term variations of daily insolation and Quaternary climatic changes, *J. Atmos. Sci.*, *35*, 2362–2367.

Black, D. E., L. C. Peterson, J. T. Overpeck, A. Kaplan, M. N. Evans, and M. Kashgarian (1999), Eight centuries of North Atlantic ocean atmosphere variability, *Science*, *286*, 1709–1713.

Black, D. E., R. C. Thunell, A. Kaplan, L. C. Peterson, and E. J. Tappa (2004), A 2000-year record of Caribbean and tropical North Atlantic hydrographic variability, *Paleoceanography*, *19*, PA2022, doi:10.1029/2003PA000982.

Bloomfield, P. (2000), *Fourier Analysis of Time Series*, 2nd ed., John Wiley, Hoboken, N. J.

Bond, G., W. Showers, M. Cheseby, R. Lotti, P. Almasi, P. deMenocal, P. Priore, H. Cullen, I. Hajdas, and G. Bonani (1997), A pervasive millennial-scale cycle in North Atlantic Holocene and glacial climates, *Science*, *278*, 1257–1266.

Box, G. E., G. M. Jenkins, and G. C. Reinsel (1994), *Time Series Analysis: Forecasting and Control*, 3rd ed., Prentice-Hall, Upper Saddle River, N. J.

Braconnot, P., O. Marti, S. Joussaume, and Y. Leclainche (2000), Ocean feedback in response to 6 kyr BP insolation, *J. Clim.*, *13*, 1537–1553.

Bradbury, J. P., B. W. Leyden, M. Salgado-Labouriau, W. M. Lewis, C. Schubert, M. W. Benford, D. G. Frey, D. R. Whitehead, and F. H. Weibezahn (1981), Late Quaternary history of Lake Valencia, Venezuela, *Science*, *214*, 1299–1305.

Carton, J. A., X. Cao, B. S. Giese, and A. M. Da Silva (1996), Decadal and interannual SST variability in the tropical Atlantic Ocean, *J. Phys. Oceanogr.*, *26*, 1165–1175.

Chang, P., J. Link, and L. Hong (1997), A decadal climate variation in the tropical Atlantic Ocean from thermodynamic air-sea interactions, *Nature*, *385*, 516–518.

Chang, P., R. Saravanan, L. Ji, and G. C. Hegerl (2000), The effect of local sea surface temperatures on atmospheric circulation over the tropical Atlantic sector, *J. Clim.*, *13*, 2195–2216.

Charles, C. D., J. Lynch-Stieglitz, U. S. Ninnemann, and R. G. Fairbanks (1996), Climate connections between the hemisphere re-

vealed by deep sea sediment core ice core correlations, *Earth Planet. Sci. Lett.*, *142*, 19–27.
Charles, C. D., D. E. Hunter, and R. G. Fairbanks (1997), Interaction between the ENSO and the Asian monsoon in a coral record of tropical climate, *Science*, *277*, 925–928.
Clement, A. C., M. A. Cane, and R. Seager (2001), An orbitally driven tropical source for abrupt climate change, *J. Clim.*, *14*, 2369–2375.
Cobb, K. M., C. D. Charles, and D. E. Hunter (2001), A central tropical Pacific coral demonstrates Pacific, Indian, and Atlantic decadal climate connections, *Geophys. Res. Lett.*, *28*, 2209–2212.
Cole, J. E., and R. G. Fairbanks (1990), The Southern Oscillation recorded in the oxygen isotopes of corals from Tarawa Atoll, *Paleoceanography*, *5*, 669–683.
Cole, J. E., R. G. Fairbanks, and G. T. Shen (1993), Recent variability in the Southern Oscillation: Isotopic results from a Tarawa atoll coral, *Science*, *260*, 1790–1793.
Corredor, J. E., and J. M. Morell (2001), Seasonal variation of physical and biogeochemical features in eastern Caribbean surface water, *J. Geophys. Res.*, *106*, 4517–4525.
Crowley, T. J., and G. R. North (1991), *Paleoclimatology*, *Oxford Monogr. Geol. Geophys.*, vol. 18, 349 pp., Oxford Univ. Press, New York.
Curtis, J. H., and D. A. Hodell (1993), An isotopic and trace element study of ostracods from Lake Miragoane, Haiti: A 10,500 year record of paleosalinity and paleotemperature changes in the Caribbean, in *Climate Change in Continental Isotopic Records*, *Geophys Monogr. Ser.*, vol. 78, edited by P. K. Swart et al., pp. 135–152, AGU, Washington, D. C.
deMenocal, P., J. Ortiz, T. Guilderson, and M. Sarnthein (2000), Coherent high- and low-latitude climate variability during the Holocene warm period, *Science*, *288*, 2198–2202.
Dong, B. W., and R. T. Sutton (2003), Variability of Atlantic Ocean heat transport and its effects on the atmosphere, *Ann. Geophys.*, *46*, 87–97.
Dunbar, R. B., and G. M. Wellington (1981), Stable isotopes in a branching coral monitor seasonal temperature variation, *Nature*, *293*, 453–455.
Dunbar, R. B., G. M. Wellington, M. W. Colgan, and P. W. Glynn (1994), Eastern Pacific sea surface temperature since 1600 AD: The $\delta^{18}O$ records of climate variability in Galapagos corals, *Paleoceanography*, *9*, 291–316.
Elsner, J. B., T. Jagger, and X. F. Niu (2000), Changes in the rates of North Atlantic major hurricane activity during the 20th century, *Geophys. Res. Lett.*, *27*, 1743–1746.
Emanuel, K. (2005), Increasing destructiveness of tropical cyclones over the past 30 years, *Nature*, *436*, 686–688.
Emrich, K., D. H. Ehhalt, and J. C. Vogel (1970), Carbon isotope fractionation during the precipitation of calcium carbonate, *Earth Planet. Sci. Lett.*, *8*, 363–371.
Enfield, D. B., and D. A. Mayer (1997), Tropical Atlantic SST variability and its relation to El Nino-Southern Oscillation, *J. Geophys. Res.*, *102*, 929–945.
Fairbanks, R. G. (1982), The origin of continental shelf and slope water in the New York Bight and Gulf of Maine: Evidence from $H_2^{18}O/H_2^{16}O$ ratio measurements, *J. Geophys. Res.*, *87*, 5796–5808.
Fairbanks, R. G., and R. E. Dodge (1979), Annual periodicity of the $^{18}O/^{16}O$ and $^{13}C/^{12}C$ ratios in the coral *Montastraea annularis*, *Geochim. Cosmochim. Acta*, *43*, 1009–1020.
Froelich, P. (1978), Influence of Amazon River discharge on surface salinity and dissolved silicate concentration in the Caribbean Sea, *Deep Sea Res.*, *25*, 735–744.
Gagan, M. K., L. K. Ayliffe, D. Hopley, J. A. Cali, G. E. Mortimer, J. Chappell, M. T. McCulloch, and M. J. Head (1998), Temperature and surface-ocean water balance of the mid-Holocene tropical western Pacific, *Science*, *279*, 1014–1018.
Gagan, M. K., L. K. Ayliffe, J. W. Beck, J. E. Cole, E. R. M. Druffel, R. B. Dunbar, and D. P. Schrag (2000), New views of tropical paleoclimates from corals, *Quat. Sci. Rev.*, *19*, 45–64.
Giannini, A., R. Saravanan, and P. Chang (2004), The preconditioning role of tropical Atlantic variability in the development of the ENSO teleconnection: Implications for the prediction of Nordeste rainfall, *Clim. Dyn.*, *22*, 839–855.
Goldenberg, S. B., C. W. Landsea, A. M. Mestas-Nunez, and W. M. Gray (2001), The recent increase in Atlantic hurricane activity: Causes and implications, *Science*, *293*, 474–480.
Gray, W. M. (1984a), Atlantic seasonal hurricane frequency: part I: El Niño and the 30 mb quasi-biennial oscillation influences, *Mon. Weather Rev.*, *112*, 1649–1668.
Gray, W. M. (1984b), Atlantic seasonal hurricane frequency: part II: Forecasting its variability, *Mon. Weather Rev.*, *112*, 1669–1683.
Gray, W. M., J. D. Sheaffer, and C. W. Landsea (1997), Climate trends associated with multidecadal variability of Atlantic hurricane activity, in *Hurricanes: Climate and Socioeconomic Impacts*, edited by H. F. Diaz and R. S. Pulwarty, pp. 15–53, Springer, New York.
Greer, L. (2001), Seasonal to centennial Holocene and modern climate variability in the Dominican Republic, Ph.D. thesis, Univ. of Miami, Miami, Fla.
Grottoli, A. G. (2001), Stable carbon isotopes ($\delta^{13}C$) in coral skeletons, *Oceanography*, *13*, 93–97.
Hakkinen, S. (2000), Decadal air-sea interaction in the North Atlantic based on observations and modeling results, *J. Clim.*, *13*, 1195–1219.
Hamelein, B., E. Bard, A. Zindler, and R. G. Fairbanks (1991), U-234/U-238 mass-spectrometry of corals—How accurate is the U-Th age of the last interglacial period?, *Earth Planet. Sci. Lett.*, *106*, 169–180.
Hastenrath, S. (1991), *Climate Dynamics of the Tropics*, 488 pp., Springer, New York.
Hastenrath, S., and L. Greischar (1993), Circulation mechanisms related to northeast Brazil rainfall anomalies, *J. Geophys. Res.*, *98*, 5093–5102.
Hastenrath, S., and P. Lamb (1977), Climatic atlas of the tropical Atlantic and eastern Pacific oceans, map, 15 pp., Univ. of Wis. Press, Madison.
Haug, G. H., K. A. Hughen, D. M. Sigman, L. C. Peterson, and U. Rohl (2001), Southward migration of the Intertropical Convergence Zone through the Holocene, *Science*, *293*, 1304–1308.
Hellweger, F. L., and A. L. Gordon (2002), Tracing Amazon River water into the Caribbean Sea, *J. Mar. Res.*, *60*, 537–549.
Higuera-Gundy, A. (1991), Antillean vegetational history and paleoclimate reconstructed from the paleolimnological record of Lake Miragoane, Haiti, Ph.D. thesis, Univ. of Florida, Gainesville.
Hodell, D. A., J. H. Curtis, G. A. Jones, A. Higuera-Gundy, M. Brenner, M. W. Binford, and K. T. Dorsey (1991), Reconstruction of Caribbean climate change over the past 10,500 years, *Nature*, *352*, 790–793.
Hodell, D. A., J. H. Curtis, and M. Brenner (1995), Possible role of climate in the collapse of Classic Maya civilization, *Nature*, *375*, 391–394.
Hu, C. M., E. T. Montgomery, R. W. Schmitt, and F. E. Muller-Karger (2004), The dispersal of the Amazon and Orinoco River water in the tropical Atlantic and Caribbean Sea: Observation from space and S-PALACE floats, *Deep Sea Res., Part II*, *51*, 1151–1171.
Huang, B. H., P. S. Schopf, and J. Shukla (2004), Intrinsic ocean-atmosphere variability of the tropical Atlantic Ocean, *J. Clim.*, *17*, 2058–2077.
Hudson, J. H. (1981), Response of *Montastrea annularis* to environmental change in the Florida Keys, in *Proceedings of the Fourth International Coral Reef Symposium*, vol. 2, pp. 233–240, Rosenstiel Sch. of Mar. and Atmos. Sci., Univ. of Miami, Miami, Fla.
Hudson, J. H., E. A. Shinn, R. B. Halley, and B. Lidz (1976), Sclerochronology—A tool for interpreting past environments, *Geology*, *4*, 360–364.
Hurrell, J. W. (1995), Decadal trends in the North Atlantic Oscillation: Regional temperature and precipitation, *Science*, *269*, 676–679.
Hurrell, J. W., and H. Vanloon (1997), Decadal variations in climate associated with the North-Atlantic Oscillation, *Clim. Change*, *36*, 301–326.
Indermuhle, A. I., et al. (1999), Holocene carbon-cycle dynamics based on CO_2 trapped in ice at Taylor Dome, Antarctica, *Nature*, *398*, 121–126.
Johnson, B. J., G. H. Miller, M. L. Fogel, J. W. Magee, M. K. Gagan, and A. R. Chivas (1999), 65,000 years of vegetation change in central Australia and the Australian summer monsoon, *Science*, *284*, 1150–1152.
Joyce, T. M., C. Deser, and M. A. Spall (2000), The relation between decadal variability of subtropical mode water and the North Atlantic Oscillation, *J. Clim.*, *13*, 2550–2569.
Joyce, T. M., C. Frankignoul, and J. Y. Yang (2004), Ocean response and feedback to the SST dipole in the tropical Atlantic, *J. Phys. Oceanogr.*, *34*, 2525–2540.
Kayano, M. T., and R. V. Andreoli (2004), Decadal variability of northern northeast Brazil rainfall and its relation to tropical sea surface temperature and global sea level pressure anomalies, *J. Geophys. Res.*, *109*, C11011, doi:10.1029/2004JC002429.
Kilbourne, K. H., T. M. Quinn, F. W. Taylor, T. Delcroix, and Y. Gouriou (2004), El Niño–Southern Oscillation–related salinity variations recorded in the skeletal geochemistry of a *Porites* coral from Espiritu Santo, Vanuatu, *Paleoceanography*, *19*, PA4002, doi:10.1029/2004PA001033.
Koopmans, L. H. (1995), *The Spectral Analysis of Time Series*, Elsevier, New York.
Koutavas, A., and J. Lynch-Stieglitz (2003), Glacial-interglacial dynamics of the eastern equatorial Pacific cold tongue-Intertropical Convergence Zone system reconstructed from oxygen isotope records, *Paleoceanography*, *18*(4), 1089, doi:10.1029/2003PA000894.
Knowlton, N., E. Weil, L. A. Weigt, and H. M. Guzman (1992), Sibling species in *Montas-*

traea-annularis, coral bleaching, and the coral climate record, *Science*, *255*, 330–333.
Kushnir, Y., R. Seager, J. Miller, and J. C. H. Chiang (2002), A simple coupled model of tropical Atlantic decadal climate variability, *Geophys. Res. Lett.*, *29*(23), 2133, doi:10.1029/2002GL015874.
Kutzbach, J. E. (1981), Monsoon climate for the early Holocene: Climate experiment with the Earth's orbital parameters for 9000 years ago, *Science*, *214*, 59–61.
Labat, D., J. Ronchail, J. Callede, J. L. Guyot, E. De Oliveira, and W. Guimaraes (2004), Wavelet analysis of Amazon hydrological regime variability, *Geophys. Res. Lett.*, *31*, L02501, doi:10.1029/2003GL018741.
Landsea, C. W. (1993), A climatology of intense (or major) Atlantic hurricanes, *Mon. Weather Rev.*, *121*, 1703–1713.
Landsea, C. W. (2005), Hurricanes and global warming, *Nature*, *438*, E11–E13.
Landsea, C. W., and W. M. Gray (1992), The strong association between western Sahelian monsoon rainfall and intense Atlantic hurricanes, *J. Clim.*, *5*, 435–453.
Landsea, C. W., W. M. Gray, P. W. Mielke, and K. J. Berry (1992), Multidecadal variations of Sahel monsoon rainfall and U.S. landfalling intense hurricanes, *J. Clim.*, *4*, 1528–1534.
Landsea, C. W., W. M. Gray, P. W. Mielke, and K. J. Berry (1994), Seasonal forecasting of Atlantic hurricane activity, *Weather*, *49*, 273–284.
Landsea, C. W., N. Nicholls, W. M. Gray, and L. A. Avila (1996), Downward trends in the frequency of Atlantic hurricanes during the past five decades, *Geophys. Res. Lett.*, *23*, 1697–1700.
Lean, J., and D. Rind (2001), Earth's Response to a variable Sun, *Science*, *292*, 234–236.
Le Bec, N., A. Juillet-Leclerc, T. Correge, D. Blamart, and T. Delcroix (2000), A coral δ^{18}O record of ENSO driven sea surface salinity variability in Fiji (south-western tropical Pacific), *Geophys. Res. Lett.*, *27*, 3897–3900.
Leder, J. J., P. K. Swart, A. Szmant, and R. E. Dodge (1996), The origin of variations in the isotopic record of Scleractinian corals: I Oxygen, *Geochim. Cosmochim. Acta*, *60*, 2857–2870.
Lighthill, J., G. Holland, W. Gray, C. Landsea, G. Craig, J. Evans, Y. Kurihara, and C. Guard (1994), Global climate change and tropical cyclones, *Bull. Am. Meteorol. Soc.*, *75*, 2147–2157.
Linsley, R. K., L. Ren, R. B. Dunbar, and S. S. Howe (2000), El Niño Southern Oscillation (ENSO) and decadal scale climate variability at 10°N in the eastern Pacific from 1893–1994: A coral-based reconstruction from Clipperton Atoll, *Paleoceanography*, *15*, 322–335.
Liu, K. B., and M. L. Fearn (2001), Reconstructions of prehistoric landfall frequencies of catastrophic hurricanes in northwestern Florida from lake sediment records, *Quat. Res.*, *54*, 238–245.
Lough, J. M., and D. J. Barnes (1990), Interannual timing of density band formation of *Porites* coral from the central Great Barrier Reef, *J. Exp. Mar. Biol. Ecol.*, *135*, 35–57.
Luckge, A., H. Doose-Rolinski, A. A. Khan, H. Schulz, and U. von Rad (2001), Monsoonal variability in the northeastern Arabian Sea during the past 5000 years: Geochemical evidence from laminated sediments, *Palaeogeogr. Palaeoclimatol. Palaeoecol.*, *167*, 273–286.
Mann, P., F. W. Taylor, R. L. Edwards, and T. L. Ku (1995), Actively evolving microplate formation by oblique collision and sideways motion along strike-slip faults: An example from the northeastern Caribbean plate margin, *Tectonophysics*, *246*, 1–69.
Marshall, J., Y. Kushnir, D. Battisti, P. Chang, A. Czaja, R. Dickson, J. Hurrell, M. McCartney, R. Saravanan, and M. Visbeck (2001), North Atlantic climate variability: Phenomena, impacts, and mechanisms, *Int. J. Clim.*, *21*, 1863–1898.
Martin, L., J. Bertaux, T. Correge, M. P. Ledru, P. Mourguiart, A. Sifeddine, F. Soubies, D. Wirrman, K. Suguio, and B. Turcq (1997), Astronomical forcing of contrasting rainfall changes in tropical South America between 12,400 and 8800 cal yr BP, *Quat. Res.*, *47*, 117–122.
Mather, J. R., H. Adams, and G. A. Yoshioka (1964), Coastal storms of the eastern United States, *J. Appl. Meteorol.*, *3*, 693–706.
McCartney, M. (1997), Climate change—Is the ocean at the helm?, *Nature*, *388*, 521–522.
Milne, P. J., and P. K. Swart (1994), Fiber-optic sensing of banded luminescence in corals, *Appl. Spectrosc.*, *48*, 1282–1284.
Molinari, R. L., and A. M. Mestas-Nuñez (2003), North Atlantic decadal variability and the formation of tropical storms and hurricanes, *Geophys. Res. Lett.*, *30*(10), 1541, doi:10.1029/2002GL016462.
Moron, V., R. Vautard, and M. Ghil (1998), Trends, interdecadal and interannual oscillations in global sea surface temperatures, *Clim. Dyn.*, *14*, 545–569.
Moses, C. S., and P. K. Swart (2006), Stable isotope and growth records in corals from the island of Tobago: Not simply a record of the Orinoco, in *Proceedings of the Tenth International Coral Reef Symposium*, in press.
Muller-Karger, F. E., P. L. Richardson, and D. McGillicuddy (1995), On the offshore dispersal of the Amazon's plume in the North Atlantic: Comments, *Deep Sea Res., Part I*, *42*, 2127–2137.
Muthiga, N. A., and A. M. Szmant (1987), The effects of salinity stress on the rates of aerobic respiration and photosynthesis in the hermatypic coral *Siderastrea Siderea*, *Biol. Bull.*, *173*, 539–551.
Neumann, C. J., B. R. Jarvinen, C. J. McAdie, and J. D. Elms (1993), *Tropical Cyclones of the North Atlantic Ocean, 1871–1992*, *Hist. Climatol. Ser.*, vol. 6-2, 193 pp., NOAA Natl. Weather Serv., Natl. Environ. Satell., Data, and Inf. Serv., Washington, D. C.
Nobre, P., and J. Shukla (1996), Variations of sea surface temperature, wind stress, and rainfall over the tropical Atlantic and South America, *J. Clim.*, *9*, 2464–2479.
Paeth, H., and A. Hense (2004), SST versus climate change signals in West African rainfall: 20th-century variations and future projections, *Clim. Change*, *65*, 179–208.
Peterson, L. C., J. T. Overpeck, N. G. Kipp, and J. Imbrie (1991), A high-resolution late Quaternary upwelling record from the anoxic Cariaco Basin, Venezuela, *Paleoceanography*, *6*, 99–119.
Philander, S. G. H., and R. C. Pacanowski (1986), A model of the seasonal cycle in the tropical Atlantic Ocean, *J. Geophys. Res.*, *91*, 14,192–14,206.
Pielke, R. A. (2005), Are there trends in hurricane destruction?, *Nature*, *438*, E11.
Piperno, D. R., M. B. Bush, and P. A. Colinaux (1990), Paleoenvironments and human occupation in late-glacial Panama, *Quat. Res.*, *33*, 108–116.
Poage, M. A., and C. P. Chamberlain (2001), Empirical relationships between elevation and the stable isotope composition of precipitation and surface waters: Considerations for studies of paleoelevation change, *Am. J. Sci.*, *301*, 1–15.
Poore, R. Z., H. J. Dowsett, S. Verardo, and T. M. Quinn (2003), Millennial- to century-scale variability in Gulf of Mexico Holocene climate records, *Paleoceanography*, *18*(2), 1048, doi:10.1029/2002PA000868.
Poore, R. Z., T. M. Quinn, and S. Verardo (2004), Century-scale movement of the Atlantic Intertropical Convergence Zone linked to solar variability, *Geophys. Res. Lett.*, *31*, L12214, doi:10.1029/2004GL019940.
Prentice, I. C., and D. Jolly (2000), Mid-Holocene and glacial-maximum vegetation geography of the northern continents and Africa, *J. Biogeogr.*, *27*, 507–519.
Quinn, T. M., F. W. Taylor, T. J. Crowley, and S. M. Link (1996), Evaluation of sampling resolution in coral stable isotope records: A case study using records from New Caledonia and Tarawa, *Paleoceanography*, *11*, 529–542.
Rind, D., and J. Overpeck (1994), Hypothesized causes of decade-to-century-scale climate variability: Climate model results, *Quat. Sci. Rev.*, *12*, 357–374.
Rodbell, D. T., G. O. Seltzer, D. M. Anderson, M. B. Abbott, D. B. Enfield, and J. H. Newman (1999), A ∼15,000-year record of El Niño-driven alluviation in southwestern Ecuador, *Science*, *283*, 516–520.
Saravanan, R., and P. Chang (2000), Interaction between tropical Atlantic variability and El Nino-Southern Oscillation, *J. Clim.*, *13*, 2177–2194.
Schubert, A. (2000), *El Lago Enriquillo: Patrimonio Natural y Cultural del Caribe*, Dir. Nac. de Parques, Pres. de la Repub., Santo Domingo, Republica Dominicana.
Seltzer, G., D. Rodbell, and S. Burns (2000), Isotopic evidence for late Quaternary climatic change in tropical South America, *Geology*, *28*, 35–38.
Slutz, R. J., S. J. Lubker, J. D. Hiscox, S. D. Woodruff, R. L. Jenne, D. H. Joseph, P. M. Steuer, and J. D. Elms (1985), Comprehensive ocean-atmosphere data set: Release 1, *Rep. NTIS PB86-105723*, 268 pp., NOAA Environ. Res. Lab., Boulder, Colo.
Stager, J. C., and P. A. Mayewski (1997), Abrupt early to mid-Holocene climatic transition registered at the equator and the poles, *Science*, *276*, 1834–1836.
Steig, E. J. (1999), Mid-Holocene climate change, *Science*, *286*, 1485–1487.
Stemann, T. A., and K. G. Johnson (1992), Coral assemblages, biofacies, and ecological zones in the mid-Holocene reef deposits of the Enriquillo Valley, Dominican Republic, *Lethaia*, *25*, 231–241.
Stern, L. A., and P. M. Blisniuk (2002), Stable isotope composition of precipitation across the southern Patagonian Andes, *J. Geophys. Res.*, *107*(D23), 4667, doi:10.1029/2002JD002509.
Sutton, R. T., and M. R. Allen (1997), Decadal predictability of North Atlantic sea surface temperature and climate, *Nature*, *388*, 563–567.
Swart, P. K., and M. L. Coleman (1980), Isotopic data for scleractinian corals explains their palaeotemperature uncertainties, *Nature*, *283*, 557–559.
Swart, P. K., and J. J. Leder (1995), Corals, paleotemperature records and the aragonite-

calcite transformation: Comment, *Geology*, *23*, 755–758.

Swart, P. K., G. F. Healy, R. E. Dodge, P. Kramer, J. H. Hudson, R. B. Halley, and M. B. Robblee (1996a), The stable oxygen and carbon isotopic record from a coral growing in Florida Bay: A 160 year record of climatic and anthropogenic influence, *Palaeogeogr. Palaeoclimatol. Palaeoecol.*, *123*, 219–237.

Swart, P. K., R. E. Dodge, and H. J. Hudson (1996b), A 240-year stable oxygen and carbon isotopic record in a coral from south Florida: Implications for the prediction of precipitation in southern Florida, *Palaios*, *11*, 362–375.

Swart, P. K., K. White, D. Enfield, R. E. Dodge, and P. Milne (1998), Corals from the Gulf of Guinea as indicators of periods of extreme precipitation conditions, *J. Geophys. Res.*, *103*, 27,885–27,891.

Swart, P. K., G. Healy, L. Greer, M. Lutz, A. Saied, D. Anderegg, R. E. Dodge, and D. Rudnick (1999), The use of proxy chemical records in coral skeletons to ascertain past environmental conditions in Florida Bay, *Estuaries*, *22*, 384–397.

Swart, P. K., R. M. Price, and L. Greer (2001), The relationship between stable isotopic variations (O, H, and C) and salinity in waters and corals from environments in South Florida: Implications for reading the paleoenvironmental record, *Bull. Am. Paleontol.*, *361*, 17–30.

Swart, P. K., A. Saied, C. Schroeder, and L. Williams (2003), Temporal and spatial variations in the oxygen isotopic compositions of surface waters from the northern Caribbean, *Eos Trans. AGU*, *84*(46), Fall Meeting Suppl., Abstract OS31C.

Tanimoto, Y., and S. P. Xie (1999), Ocean-atmosphere variability over the Pan-Atlantic basin, *J. Meteorol. Soc. Jpn.*, *77*, 31–46.

Tanimoto, Y., and S. P. Xie (2002), Inter-hemispheric decadal variations in SST, surface wind, heat flux and cloud cover over the Atlantic Ocean, *J. Meteorol. Soc. Jpn.*, *80*, 1199–1219.

Taylor, F. W., P. Mann, S. Valastro, and K. Burke (1985), Stratigraphy and radiocarbon chronology of a subaerially exposed Holocene coral reef, Dominican Republic, *J. Geol.*, *93*, 311–332.

Tedesco, K., and R. Thunell (2003), High resolution tropical climate record for the last 6,000 years, *Geophys. Res. Lett.*, *30*(17), 1891, doi:10.1029/2003GL017959.

Trenberth, K. (2005), Uncertainty in hurricanes and global warming, *Science*, *308*, 1753–1754.

Tudhope, A. W., C. P. Chilcott, M. T. McColluch, E. R. Cook, J. Chappell, R. M. Ellam, D. W. Lea, J. M. Lough, and G. B. Shimmield (2001), Variability in the El Niño-Southern Oscillation through a glacial-interglacial cycle, *Science*, *291*, 1511–1517.

Wang, C., and D. B. Enfield (2001), The tropical Western Hemisphere warm pool, *Geophys. Res. Lett.*, *28*, 1635–1638.

Warner, R. M. (1998), *Spectral Analysis of Time-Series Data*, Guilford Press, New York.

Watanabe, T., A. Winter, T. Oba, R. Anzai, and H. Ishioroshi (2002), Evaluation of the fidelity of isotope records as an environmental proxy in the coral *Montastrea*, *Coral Reefs*, *21*, 169–178.

Weber, J. N., and P. M. J. Woodhead (1972), Temperature dependence of oxygen-18 concentration in reef coral carbonates, *J. Geophys. Res.*, *77*, 463–473.

Webster, P. J., G. J. Holland, J. A. Curry, and H. R. Chang (2005), Changes in tropical cyclone number, duration, and intensity in a warming environment, *Science*, *309*, 1844–1846.

Xie, L., L. J. Pietrafesa, and K. J. Wu (2002), Interannual and decadal variability of landfalling tropical cyclones in the southeast coastal states of the United States, *Adv. Atmos. Sci.*, *19*, 677–686.

Xie, S. P., and Y. Tanimoto (1998), A pan-Atlantic decadal climate oscillation, *Geophys. Res. Lett.*, *25*, 2185–2188.

Zhang, K., B. C. Douglas, and S. P. Leatherman (2000), Twentieth-century storm activity along the U.S. east coast, *J. Clim.*, *13*, 1748–1761.

L. Greer, Department of Geology, Washington and Lee University, Lexington, VA 24450-0303, USA. (greerl@wlu.edu)

P. K. Swart, Rosenstiel School of Marine and Atmospheric Science, University of Miami, 4600 Rickenbacker Causeway, Miami, FL 33149-1003, USA.